

Importance of dense aquatic vegetation in seasonal phosphate and particle transport in an
agricultural headwater stream.

Thesis

Presented in Partial Fulfillment of the Requirements for the Degree Master Science in the
Graduate School of The Ohio State University

By

Hannah Ruth Field, B.S.

Graduate Program in Earth Sciences

The Ohio State University

2022

Thesis Committee

Dr. Audrey Sawyer, Advisor

Dr. James Hood

Dr. Gil Bohrer

Copyrighted by
Hannah Ruth Field
2022

Abstract

Agricultural headwater ditches and streams are frequently maintained by removing woody riparian vegetation, leading to seasonal growth of aquatic vegetation that influences the transport of water and nutrients from cropland to larger rivers. This study examined seasonal changes in the transport of phosphorus (P) in an agricultural drainage ditch in the Maumee River Basin (Ohio, USA) by conducting constant rate injections of a novel tracer mixture [conservative salt (Cl as NaCl), dissolved P (KH_2PO_4), and a fluorescent fine particle (Dayglo AX-11-5 Aurora Pink®)] in spring, summer, and fall as aquatic vegetation grew and decayed. I modeled retention and transport behavior for solutes and particles using a traditional transient storage approach consisting of mobile and immobile storage zones, connected by a first-order exchange rate constant. Transient storage of solutes and particles was greatest during the spring, when thicker vegetation stands caused more pooling and flow stagnation, while transient storage decreased through fall as reed grasses decayed and vegetation stands became thinner and smaller. Nutrient spiraling lengths were 8.7 times longer in fall than spring, likely due to declines in both biological uptake rates with fall senescence and transient storage in shrinking vegetation stands. With the increasing eutrophication of major waterbodies like Lake Erie and the Gulf of Mexico, it is crucial to better understand how nutrients move through agricultural headwater systems. This study highlights the physical and biological roles of aquatic vegetation in creating immobile zones that slow the downstream movement of nutrients, increasing the assimilation of dissolved nutrients, and filtering particle-bound nutrients. Because these processes are seasonal, the relationships between travel times of soluble and particle-bound nutrients are also strongly seasonal, with the greatest disparity in travel times occurring in the spring, when nutrient export is typically greatest.

Acknowledgements

This work was supported by funding through the USDA-NRCS Conservation Effects Assessment Project in collaboration with the USDA-Agricultural Research Service. I also received funding from The Geological Society of America Graduate Student Research Grant, and The American Geosciences Institute Harriet Evelyn Wallace Scholarship. Thank you to The Ohio State University School of Earth Sciences for Graduate Teaching support.

I want to thank my advisor, Dr. Audrey Sawyer, for the continuous support and encouragement that has cultivated my evolution as a graduate student. She constantly challenged me to grow as both a scientist and person and always made herself available for feedback and advice, no matter the circumstances. Her consistent belief in me has pushed me to achieve more than I imagined I could in two short years. I also want to thank my committee members, Dr. Gil Bohrer and Dr. Jim Hood, for their insightful feedback that has strengthened this study.

I am very grateful for the unyielding support of the undergraduate researchers in my research group during my fieldwork. A special thanks to Ryan Benefiel and Bri Tomko, who would get up before dawn and work until the day (or night) was finished on long field days. This project would not have been possible without the assistance of my fieldwork crews, including Lauren Decker, Kat Meiner, Harper Luckeydoo, Ian Gilles, and Mary Kate Rinderle, who spent long days sampling in sun, rain, and freezing conditions.

I am very grateful for the guidance of Dr. Sue Welch, who has contributed greatly to the laboratory analyses during my masters work. I would also like to thank Dr. Zackary Johnson at Duke University's Marine Laboratory, who contributed great expertise to designing and conducting the measurement of particle counts using flow cytometry. I also greatly appreciate

the feedback and guidance provided by Dr. Brittany Hanrahan, Dr. Rebecca Kreiling, and Dr. Kevin King in the conception and approach to experimental design. The insight provided by Dr. Diana Karwan and Ethan Pawlowski at the University of Minnesota was also invaluable in designing my experiments.

And finally, I am deeply thankful for the constant support of my friends, fellow graduate students, and siblings, who acted as moral support throughout my journey.

Author Contributions

Hannah Field and Audrey Sawyer designed experiments. Hannah Field led all field experiments and analyzed phosphorus, chloride, and fine particle concentrations under the guidance of Sue Welch and Zackary Johnson. Hannah Field modeled the results with the guidance of Audrey Sawyer and wrote the thesis, with suggestions from Audrey Sawyer and thesis committee members.

Vita

- 2020 Bachelor of Science, Geology, Appalachian State University, Boone, NC.
- 2018 – 2020 Undergraduate Research Assistant, Department of Earth and Environmental Sciences, Appalachian State University, Boone, NC.
- 2018 NSF REU Intern, Department of Crop and Soil Sciences, North Carolina State University, Raleigh, NC.
- 2020 – present Graduate Research Associate, The Ohio State University, Columbus, OH.
- 2021 Directorate Fellow, U.S. Fish and Wildlife Service, Albuquerque, NM.

Publications

Field, H. R., Armstrong, W. H., and Huss, M. Topography exerts primary control on the rate of Gulf of Alaska ice-marginal lakes over the Landsat record: The Cryosphere.

<https://tc.copernicus.org/articles/15/3255/2021/>

Field, H. R., Whitaker, A. H., Henson, J. A., and Duckworth, O. W., 2019, Sorption of copper and phosphate to diverse biogenic iron (oxyhydr) oxide deposits: Science of The Total Environment, p. 134111. <https://doi.org/10.1016/j.scitotenv.2019.134111>

Fields of Study

Major Field: Earth Sciences

Table of Contents

Abstract.....	ii
Acknowledgements.....	iii
Author Contributions.....	iv
Vita.....	v
List of Tables.....	vii
List of Figures.....	viii
Chapter 1. Importance of dense aquatic vegetation in seasonal phosphate and particle transport in an agricultural headwater stream.....	1
Bibliography.....	34
Appendix A. Solute and fine particle concentrations observed at the upstream sampling station (26 m) during the May injection experiment.....	40
Appendix B. Solute and fine particle concentrations observed at the downstream sampling station (92 m) during the May injection experiment.....	41
Appendix C. Solute and fine particle concentrations observed at the upstream sampling station (26 m) during the July injection experiment.....	42
Appendix D. Solute and fine particle concentrations observed at the downstream sampling station (92 m) during the July injection experiment.....	43
Appendix E. Solute and fine particle concentrations observed at the upstream sampling station (26 m) during the December injection experiment.....	44
Appendix F. Solute and fine particle concentrations observed at the downstream sampling station (92 m) during the December injection experiment.....	45
Appendix H. Particle distribution between sediment and vegetation.....	46

List of Tables

Table 1. Details of continuous spring (May), summer (July), and fall (December) stream injections.

Table 2. Average physical and chemical stream measurements during respective spring (May), summer (July), and fall (December) nutrient additions. May pH, oxidation-reduction potential, and dissolved oxygen measurements were made using an unfiltered 1-L water sample collected in the field and transport back to the lab on ice, while July and December water quality measurements were made in the field. b.d. = below detection (0.001 mg/L).

Table 3. Nutrient and fine particle uptake and filtration metrics.

Table 4. Best fit parameters for OTIS simulations for conservative (Cl tracer) transport in the experimental reach observed during each season.

Table 5. Best fit parameters for nonconservative removal of SRP and fine particles.

List of Figures

Figure 1. Conceptualization of aquatic vegetation on fine particle transport and sources of P uptake.

Figure 2. A) Site location and downstream flow path to Lake Erie. B) Stream site location and local headwaters exhibiting linear channel C) Map of the experimental reach, injection location, and sampling stations. The model reach lies between station 1 and 3. Other stations were used only for dilution gauging and nutrient uptake estimates.

Figure 3. Stream site conditions in (A) May, (B) July, and (C) December, illustrating emergent vegetation stands in spring, mature vegetation in the summer, and the die off and decay of vegetation in the fall.

Figure 4. Schematic of compartments and processes incorporated in the OTIS model.

Figure 5. Particle size fractions of streambed sediment in each season.

Figure 6. (A) SRP uptake velocity and fine particle uptake velocity, (B) spiraling lengths, and (C) storage area to total stream channel area fraction.

Figure 7. OTIS fits for Cl, P, and fine particles for the May injection (A-C), July injection (D-F), and December injection (G-I).

Figure 8. Estimated fraction of total particles retained in either the sediment or vegetation after each injection.

Chapter 1. Importance of dense aquatic vegetation in seasonal phosphate and particle transport in an agricultural headwater stream

Introduction

Water management in the midwestern United States is dominated by artificial drainage networks that consist of subsurface tile drains, surface drainage ditches, and channelized streams (McCorvie and Lant, 1993). Flat topography and poorly drained soils necessitated the construction of these artificial drainage networks to support cropland expansion and removal of excess water, resulting in increased yield (Myers et al., 2000). These drainage networks have helped expand productive agriculture while also immensely altering hydrological regimes and nutrient export (McCorvie and Lant, 1993; Smith, 2009). Subsurface tile drains increase overall discharge (King et al., 2014) and contribute large nutrient and sediment loads to streams (Schilling and Helmers, 2008). Woody vegetation along agricultural headwater streams is often removed because it impedes flow and contributes to blockages (Needelman et al., 2007). In the absence of shade from a woody canopy, dense aquatic vegetation flourishes in channels and riparian zones. The aquatic vegetation leads to differences in nutrient transport (Sweeney and Newbold, 2014) by creating transient storage zones that retain solutes (Bohrman and Strauss, 2018; Nepf, 2012), increasing biological assimilation (by both the plants themselves and biofilms growing on plants), and trapping fine particles that sorb nutrients (Barko et al., 1991; Carignan, 1982; Huang et al., 2008).

Nutrient dynamics within these modified agricultural headwater streams are essential to consider, given the increasing severity of harmful algal blooms in major waterbodies like Lake Erie (Jankowiak et al., 2019) and the Gulf of Mexico (Rabalais and Turner, 2019). Headwater streams function as the link between cropland and larger streams and rivers (Kincaid et al., 2020). They are pervasive and collectively account for the majority of total stream length in

watersheds (Horton, 1945; Nadeau and Rains, 2007). As a result, the export of legacy nutrients that have accumulated in the landscape depends partly on whether headwater streams act as nutrient sources or sinks (Basu et al., 2010; Hoffman et al., 2009). An understanding of nutrient transport in headwater streams is also critical for guiding conservation management that seeks to balance effective crop production with environmental stewardship (Smith et al., 2018).

In the case of phosphorus (P), a large portion of P transport occurs in particulate form, since soluble reactive P (SRP) has a high sorption affinity for metal-oxides and clay particulates (Baken et al., 2016; Froelich, 1988; House et al., 2007) (Figure 1). The mobilization of particulates can contribute greatly to the downstream transport of total P in streams, especially in agricultural settings, and aquatic vegetation can reduce this downstream transport (de Jonge et al., 2004). Particles and their associated P can be retained in the stream bed and on aquatic vegetation. SRP can sorb to and desorb from sediment, be taken up by microbes and plants, or follow slow flow paths through bed sediments and aquatic vegetation stands (Drummond et al., 2020, 2017; Harvey et al., 2012). Thus, investigating the dynamics and drivers of both fine particle and SRP movement is important for understanding how aquatic vegetation and other agricultural stream characteristics impact the transport and fate of various form of P.

A growing number of studies have examined soluble nutrient transport (Bernot et al., 2006; Famularo, 2019; Macrae et al., 2003; Weigelhofer, 2017) or fine particle transport (Drummond et al., 2014; Harvey et al., 2012) in agricultural headwater streams. Small agricultural streams are generally subject to higher nutrient concentrations in stream water and bed sediment than small forested streams (Bernot et al., 2006; Macrae et al., 2003; Vaughan et al., 2007) and more rapidly accumulate fine particles (Blann et al., 2009; Brueske and Barrett, 1994). Studies of soluble P have shown that stream SRP concentrations influence the rate of

uptake and that biologically mediated SRP uptake is greater in agricultural streams than forested streams (Bernot et al., 2006). Deforested agricultural streams also experience much greater fine particle mobilization than their forested counterparts (Hobbie and Likens, 1973), but in-channel vegetation presence can facilitate greater sediment deposition and storage (Brueske and Barrett, 1994). Based on pore water extractions, Casillas-Ituarte et al. (2020) suggested that agricultural drainage ditch sediments can act as a persistent source of dissolved P to downstream reaches and may account for roughly one-tenth of all dissolved P export from the watershed. It is thus critical to explore the movement of both dissolved P and sediments holistically in agricultural streams (Hobbie and Likens, 1973; Wu et al., 2014; Yu et al., 2022).

One tool that has been powerful for understanding both solute and particle movement is continuous tracer injections (Drummond et al., 2014; Harvey et al., 2012; Macrae et al., 2003; Smith, 2009). Continuous injections can be an effective approach for estimating nutrient uptake rates (Powers et al., 2009; Trentman et al., 2015). They are also more effective than pulse injections for determining longer timescales of solute retention in transient storage zones (Harvey and Wagner, 1997). Many studies employ continuous injections to investigate how SRP (Burrows et al., 2013; Macrae et al., 2003; Mulholland et al., 1990) or fine particles (Drummond et al., 2020; Harvey et al., 2012; Minshall et al., 2000) are transported in various stream environments. This work aims to extend past tracer experimental methods for P in agricultural streams by co-injecting both SRP and particles and describing their transport behavior using the classical OTIS model (Runkel, 1998). The goal of this study was to understand transport behavior under similar flow conditions throughout different seasons. I hypothesized that the retention of SRP and fine particles would be greatest in the spring and summer when dense

vegetation promotes transient storage and provides surfaces for biofilm growth and would decline in the fall as vegetation becomes thin.

Methods

Site Description

I conducted this study in an unnamed, first-order tributary of the Little Auglaize River in the Auglaize watershed in the Lake Erie Basin (Figure 2A). The site is adjacent to a USDA-ARS edge-of-field study designed to investigate the impacts of crop production and conservation practices (Williams et al., 2016).

The study reach is 66 m long and consists of narrow, shallow runs and deeper pools. Flow depths ranged from 13.7 – 16.5 cm and width ranged from 0.37 – 1.14 m over the three seasons (Figure 2C; Figure 3). The streambed is dominated by silt and clay. The channel slope of the study reach is approximately 0.5% and was derived using Ohio Statewide Imagery Program (OSIP) LiDAR data (<https://gis5.oit.ohio.gov/geodatadownload/>). The stream is dominated by monotypic stands of grass in the spring and summer (Figure 3A – 3B). In the fall, masses of dead vegetation (predominantly grasses) are prominent (Figure 3C). Visual observations indicate that the extensive presence of grass in all seasons influences flow characteristics of the stream, similar to other agricultural stream sites (Gebauer et al., 2012). Vegetation also alters channel morphology, particularly where extensive mats of grass create narrow runs or choke the channel entirely and redirect the flow.

Sample Collection and Analysis

I conducted constant rate injections of NaCl, KH₂PO₄, and Dayglo® fluorescent particles (average diameter ~ 4 μm) in each of three seasons. Incorporating 5 g/L of a dispersant (Na₆(PO₃)₆, henceforth referred to as SHMP) facilitated complete mixing of the slightly

hydrophobic Dayglo® fluorescent particles (Drummond et al., 2017; Harvey et al., 2012). I estimated the target concentration of KH_2PO_4 in the injectate based on measured background concentrations of SRP in the stream that were made one to two days prior to the injection using a handheld CHEMetrics V-2000 Multi-Analyte Photometer (Midland, VA). I premixed the solution in a single container and introduced it to the stream via a singular drip. I increased the concentration of Dayglo relative to KH_2PO_4 in the second and third seasons to account for substantial retention that I observed in the first season (Table 1). Ratios between the tracers in the injectate therefore varied by up to 83% among seasons. The duration of each release depended on streamflow and ranged from 60 – 100 minutes among seasons (Table 1).

I established the start of the experimental reach (sampling station 1; Figure 2C) 26 m downstream of the injection location to allow for adequate tracer mixing based on prior NaCl injections I conducted in the reach. Subsequent sampling stations were located at 44 m, 66 m, and 166 m from station 1. I employed continuous in-stream electrical conductivity monitoring at sampling stations using In-Situ AquaTROLL sensors at a 1-min sampling interval. I used a YSI ProQuatro Multiparameter device to monitor real-time water quality at various times and locations to inform sampling frequency. I adjusted sampling frequency of grab samples for Cl, SRP, and fine particles from every 2 – 5 minutes during the times of rising and falling concentrations to every 10 – 30 minutes during the plateau and at late times in the tail of the breakthrough curve based on real-time observations of specific conductivity using the multiparameter device. Each grab samples was collected using 30 mL polypropylene syringes and split into one unfiltered and one filtered ($0.45\ \mu\text{m}$) aliquot. Samples were immediately placed on ice and transferred to a refrigerator upon return to the analytical laboratory (within 12 hours). Filtered aliquots were analyzed for Cl using ion chromatography and for SRP using a

Skalar SAN++ nutrient analyzer within 2-4 weeks of collection. SRP analyses followed the acid-molybdenum-blue colorimetric method (APHA, 1998). A subset of unfiltered samples from the fall experiment was analyzed for total P on a Skalar SAN++ nutrient analyzer using the acid persulfate digestion method and were run within 1 week of sample collection. Fine particle analysis was conducted with an Attune NxT Flow Cytometer (Environmental Cytometry Facility, Johnson Lab at the Duke Marine Laboratory, Beaufort, North Carolina) and FlowJo software using the 405 nm, 488 nm, and 637 nm lasers.

In order to estimate particle retention on vegetation and in streambed sediments, I collected vegetation and sediment samples 8 - 25 hours after the end of each injection, once surface water sampling concluded. I collected sediment cores to a depth of 5 cm using a 7.62 cm diameter clear PVC pipe along the reach at 3 locations in the spring and 5 locations in the summer and fall. At the same sample locations (within 1 - 2 m), I used a PVC quadrat (0.5 m x 0.5 m) to cut and discard vegetation above the water surface and then cut remaining vegetation as close to the streambed as possible, while minimizing particle mobilization. Sampled vegetation was stored in sealable plastic bags.

To characterize changes in vegetation stands across seasons, I also surveyed the proportion of the vertical channel cross-section blocked by vegetation stands in 12 - 18 locations along the experimental reach after each tracer test. Additionally, I determined stem counts and diameters within the quadrat where I sampled vegetation for particles.

Sediment cores were homogenized, and a Falcon tube was used to acquire a plug of approximately 15 mL of the homogenized sediment. The subsample was weighed and then mixed into 35 mL of DI water. Particle counts were determined using black-gridded microscope slides with a fluorescent microscope using the blue light (480 nm), which excites the particle

fluorescence. No staining was necessary. To determine particle content on vegetation, 250 mL of a 5 g/L SHMP solution was added to vegetation sample bags. The samples were shaken vigorously in the sealable plastic bags and decanted into HDPE plastic sample bottles and refrigerated until particle counts were obtained.

To characterize changes in streambed sediments across seasons, I also collected three cores within 5 m of each other in a pool above the mixing reach to be analyzed for physical and chemical sediment characteristics. Sediment core samples were oven-dried at 105 °C to calculate moisture content, bulk density, total porosity, and water-filled pore space (Robertson et al., 1999). Then, dried sediment was ashed in a muffle furnace for 3 hr at 450°C to determine the percentage of volatile solids (Robertson et al., 1999). Particle size distribution was measured with the integral suspension pressure method (Durner and Iden, 2021). Particle classes included coarse sand (630–2000 µm), middle sand (200–630 µm), fine sand (63–200 µm), coarse silt (20–63 µm), middle silt (6.3–20 µm), fine silt (2.0–6.3 µm) and clay (< 2.0 µm).

The potential for the streambed sediment to bind or release P can be measured with the equilibrium P concentration (EPC_0), which is the concentration of dissolved P at which minimal P uptake or release from sediment occurs (Froelich, 1988). To measure EPC_0 , approximately 1.5 g of wet sediment was added to each of six 50-mL centrifuge tubes along with 30 mL 0.01 M KCl solution enriched with P concentrations of 2.0, 1.0, 0.1, 0.05, and 0 mg P/L (Kreiling et al., 2019). The samples were shaken for 24 hours at room temperature and then centrifuged at 2900 RPM. The resulting supernatant was filtered through a 0.45-µm filter and analyzed for SRP using the ascorbic acid method (Standard Method 4500-PE; APHA et al., 2017). A linear regression of the amount of P sorbed onto the sediment (mg P/kg dry sediment) versus the

remaining SRP concentration (mg P/L) in the water fraction in the centrifuge tubes was used to determine the EPC₀, which was the x-intercept in the regression equation.

Stream Discharge and Tracer Mass Balance

Streamflow discharge (Q) was estimated using observed injection rates, measured Cl injectate concentrations, and observed Cl concentrations at downstream sampling locations during the injection plateau, following USGS methods described in Capesius et al (2005). Mass balances for solutes and fine particles were calculated by integrating the concentration timeseries.

Modeling

I employed the USGS OTIS model to estimate solute and particle transport characteristics in each season (Bencala and Walters, 1983; Runkel, 1998; Runkel et al., 2005). The OTIS model is governed by a one-dimensional advection-dispersion equation with a mobile zone, where advection and dispersion occur, and an immobile storage zone, where no advection and dispersion occur (Figure 4). Specifically:

$$Eq. 1 \quad \frac{\partial C}{\partial t} = -\frac{Q}{A} \frac{\partial C}{\partial x} + \frac{1}{A} \frac{\partial}{\partial x} \left(AD \frac{\partial C}{\partial x} \right) + \frac{q_{Lin}}{A} (C_L - C) + \alpha (C_I - C) \pm R$$

$$Eq. 2 \quad \frac{dC_I}{dt} = \alpha \frac{A}{A_I} (C - C_I) \pm R_I,$$

where Q [L^3/T where L = units of length and T = units of time] is streamflow discharge, C [M/L^3 where M = units of mass] is the concentration of the solute in the mobile zone, x [L] is the reach length of the stream, q_{Lin} is the lateral influx of water with solute concentration C_L , A [L^2] is the vertical cross-sectional area of the mobile zone in the stream channel, A_I [L^2] is the vertical cross-sectional area of the immobile storage zone, D [L^2/T] is the dispersion coefficient, t [T] is time, α [$1/T$] is the exchange coefficient between mobile and immobile storage zones, and R and R_I represent non-conservative processes in the mobile and immobile zones [$M/L^3/T$]. Because in-

stream plateau concentrations indicate that there was negligible lateral inflow in the stream reach, I assume that $q_{Lin} = 0$. I fit physical transport parameters (α , A , A_I , D , Q) using the conservative solute (Cl) and then fit non-conservative parameters for SRP and fine particles (R and R_I). In the case of conservative tracers (chloride), R and R_I are zero. In the case of non-conservative tracers (SRP and fine particles):

$$Eq. 3 \quad R = \rho \hat{\lambda} (S - K_d C) - \lambda C, \text{ and}$$

$$Eq. 4 \quad R_I = \hat{\lambda}_I (\hat{C}_I - C_I) - \lambda_I C_I.$$

The first term in Eqs. 3 and 4 describes reversible sorption on solid matter, where \hat{C}_I [M/L³] is the concentration in the immobile zone before the experiment, C_I [M/L³] is the solute concentration in the immobile zone, ρ [M/L³] is the ratio of accessible solid mass to volume of water, $\hat{\lambda}$ [1/T] is the sorption rate coefficient in the mobile zone, S [M/L³] is the sorbate concentration on solid matter, and K_d [L³/M] is the distribution coefficient, which describes partitioning between the dissolved and sorbed phases at equilibrium. In Eq. 4, $\hat{\lambda}_I$ [1/T] is the sorption rate coefficient in the immobile storage zone. Because of the fine texture of the streambed, I assumed hyporheic exchange was minimal and that vegetation stands and stagnant pools contributed to most of the immobile zone storage at the site. I therefore assumed similar sorption kinetics for SRP in the mobile and immobile zones ($\hat{\lambda} = \hat{\lambda}_I$). S is given by:

$$Eq. 5 \quad \frac{dS}{dt} = \hat{\lambda}(K_d C - S).$$

The second term in Eqs. 3 and 4 represents any removal process with first-order kinetic rate constant λ [1/T] or λ_I [1/T] for the mobile or immobile zone, respectively. In the case of SRP, removal primarily represents plant, sediment, and stream biota uptake (Bernot et al., 2006; Trentman et al., 2020). To discern whether sorption ($\hat{\lambda}$ and $\hat{\lambda}_I$) or uptake (λ and λ_I) dominates

overall SRP removal processes, I fit models with exclusively sorption, exclusively uptake, and combinations of both sorption and uptake to determine the best fitting option.

In the case of fine particles, removal is assumed to occur primarily due to deposition and filtration in either vegetation or the porous streambed, both of which can occur in either mobile or immobile zones. Because of the fine texture of the streambed and presence of dense aquatic vegetation, I assume most filtration occurs on plant stems rather than along hyporheic flow paths. The filtration of particles on aquatic vegetation has previously been parameterized as a first-order kinetic rate process (Huang et al., 2008; Saiers et al., 2003; Wu et al., 2014; Yu et al., 2022), where the first-order rate constant for particle capture is related to a dimensionless particle capture efficiency, η , conceptualized as the rate particles are captured by a single stem relative to the rate they approach the stem (Wu et al., 2011, 2012). Here, I adopt a modified version η^* , which represents the rate particles are captured by a single stem relative to the rate they flow downstream through the mobile zone, as there is no advection in the immobile zone. Specifically:

$$Eq. 6 \quad \eta^* = \frac{\lambda_I(1-ad)}{au},$$

where a is the stem frontal area per unit stream channel volume (L^{-1}), d is the average vegetation stem diameter (L), and the term ad represents the vegetation volume fraction (Huang et al., 2008). In this case, u is the velocity in the mobile stream zone. While more complex parameterizations of η exist that account for physical processes such as van der Waals attraction, electrostatic double layer repulsion, and hydrodynamic shear interactions, the simplified formulation in Eq. 6 is harmonious with the OTIS model and has been adopted in previous studies (Huang et al., 2008; Wu et al., 2011, 2012; Yu et al., 2022). I first estimated λ_I by fitting the OTIS model with particle breakthrough curves and then calculated η^* using Eq 6 and

observations of stem diameters from quadrant samples and stem frontal areas at cross-sections. For comparison, I also estimated η^* using the conceptual definition and measured particle counts on vegetation samples. Effectively, I determined the average number of particles captured per stem in the vegetation samples, and I divided this value by the total number of particles I released downstream.

Results

Stream conditions

Stream discharge was greatest during the spring injection (13.0 L/s), intermediate in the summer season (9.6 L/s) and least during the fall season (4.7 L/s). Aquatic vegetation stands (Figure 3) blocked an average of 25.3% (SD = 18.9%) of the channel cross-sectional area in spring, 17.1% (SD = 21.8%) in summer, and 31.1% (SD = 24.9%) in fall. Although the stands were more aerially expansive in fall, stems were fallen and decaying. The total submerged vegetation volume fraction for the reach was therefore greatest in spring ($6.50 \times 10^{-4} \text{ m}^{-1} \pm 3.34 \times 10^{-5} \text{ m}$) and lesser in summer ($3.15 \times 10^{-4} \text{ m}^{-1} \pm 7.42 \times 10^{-5} \text{ m}^{-1}$) and fall ($4.08 \times 10^{-5} \text{ m}^{-1} \pm 2.64 \times 10^{-4}$).

During the spring injection, the streambed sediment sample characterized for sediment composition contained a lesser fraction of clay (28.3%) and greater fraction of sand (40.1%) than in other seasons (Figure 5). EPC_0 was relatively low (0.002 – 0.012 mg/L) for streambed sediment but was greater than the measured stream water SRP concentrations indicating potential P release from the sediment (Table 2). Therefore, when the stream water SRP concentration was raised above the EPC_0 during the injections, the streambed sediment had the potential to transition from acting as a source of P to acting as a sink of P (Reddy et al., 1999).

Solute and Particle Transport

The mass balance between the upstream and downstream sampling locations indicates that during the spring injection, nearly all of the conservative tracer (Cl) was recovered (99%) in the reach, however, the mass recovery during the summer and fall seasons appeared to exceed complete recovery (104 and 117%, respectively), indicating the potential presence of tile drainage inputs that may have acted as an additional source of Cl, particularly in fall. I observed two tile drains along the reach that were not flowing and one submerged outlet from a surface collector that may have contributed an immeasurably small amount of discharge.

In the case of SRP, 69% of the mass flux at the first station was recovered at the third station in the spring, indicating retention of nearly one-third of the added SRP over the timescale of the experiment. In the summer and fall, essentially complete recovery (99%) was observed, indicating no substantial retention. The stream retained 95% of particles in the spring and over half (54 and 52%) of the particles during the summer and fall injections.

The fastest SRP uptake velocity (calculated from plateau concentrations at multiple downstream sampling sites) occurred in the spring ($V_f = 0.22 \text{ mm sec}^{-1}$) and decreased in the summer ($V_f = 0.028 \text{ mm sec}^{-1}$) and fall ($V_f = 0.008 \text{ mm sec}^{-1}$) (Figure 6). A similar trend was observed for the fine particle uptake velocity, with spring being the fastest ($V_f = 0.74 \text{ mm sec}^{-1}$), and decreasing in the summer ($0.065 \text{ mm sec}^{-1}$) and fall (0.54 mm sec^{-1}). Examining kinetic parameters derived from OTIS models, the fastest SRP uptake rate coefficient (λ, λ_f) was observed in the spring. Similarly, the model-derived particle removal rate coefficient describing particle filtration on vegetation (λ, λ_f) was greatest in the spring and decreased in the summer and fall (Table 3). It is worth noting that a combination of both uptake and sorption was needed to fit the late-time tailing behavior for SRP in spring (Table 5). In the summer and fall, late-time tailing behavior in SRP was best fit by implementing uptake only.

In spring, the strong removal kinetics for both SRP and particles coincided with greater immobile zone storage. Specifically, the relative size of the immobile zone, or the ratio of the immobile zone to total stream cross-sectional area ($A_I/(A+A_I)$); Figure 6; Table 3; Table 4), was greatest in spring. The exchange rate (α) between the stream channel, A , and storage zone, A_I , was also fastest in the spring ($\alpha = 0.01 \text{ sec}^{-1}$). As a result, the residence time of conservative solute within the immobile zone, $T_{sto} = A_s/\alpha A$, was shortest in the spring by over an order of magnitude, meaning that water moved quickly in and out of the relatively large immobile storage zone and did not reside there long. The conservative spiraling length, ($L_s = u/\alpha$) which represents the average distance that solute travels in the mobile zone before entering the immobile zone (Harvey and Wagner, 2000), was shorter by almost an order of magnitude in spring, indicating more efficient turnover of solutes and suspended particles between mobile and immobile zones. Uptake lengths, S_w (Table 3), for SRP and fine particles were both shortest in spring. S_w for SRP was 70.1 – 87.5% longer than S_w for fine particles across all three seasons.

Overall, the transient storage model captured trends in breakthrough behavior for the injected solutes, though the recovery in the tail of the falling limb was generally overestimated slightly for chloride and underestimated for SRP (Figure 7). In the case of particles, the model fit was weaker, particularly in spring. Following the spring injection, light showers occurred approximately 205 minutes into the experiment. Though small, these showers may have contributed to difficulties fitting the model to the observed breakthrough curves.

The homogenized concentrations of particles in soil cores was greatest in the fall ($2.44 \times 10^4 \text{ particles/cm}^3$) and spring ($1.24 \times 10^4 \text{ particles/cm}^3$), and least in the summer ($1.98 \times 10^3 \text{ particles/cm}^3$). Assuming that core samples are representative of particle deposition rates across the entire wetted streambed and that vegetation samples are representative of particle capture

throughout all vegetation stands in the reach, greater particle retention occurred on vegetation than at the sediment-water interface in the spring (Figure 8; Appendix H). Conversely, in the fall, the proportion of total particles retained by vegetation was less than the total particles retained in sediment, and this is reflected by the observed single stem removal efficiency, η^* , being least in the fall (0.005%), compared to spring (0.015%), and summer (0.010%).

Discussion

Aquatic vegetation plays an important role in both dissolved and particulate P transport in agricultural headwater streams, particularly in spring. Roughly 31% of the SRP and 95% of the fine particles were retained within the reach during the spring season when dense vegetation was actively emerging and acting as an uptake mechanism for SRP and an effective physical filter for fine particles (Ky et al., 2020; O'Brien et al., 2014). Vegetation influences nutrient retention through two mechanisms. First, it increases hydrologic connectivity between mobile and immobile zones, increasing travel times and creating more opportunity for removal of dissolved nutrients and deposition of particles along flow paths (Figure 4). In spring, the growth of dense stands interacted more with the faster current and facilitated greater exchange between the mobile stream channel and immobile stands (α , Table 4). The net result was that a greater proportion of water exchanged through the immobile storage zone and the turnover length (L_s) was much shorter, despite greater stream discharge in spring. Second, vegetation contributes to greater removal kinetics (Table 5). Here, the first-order uptake rate constant for SRP (λ , λ_I) and the first-order filtration rate constant for particles (λ , λ_I) were all greater during the spring season when vegetation was dense. Denser vegetation traps particles (Fauria et al., 2015; Yu et al., 2022) and provides a substrate for biofilms that contribute to dissolved P uptake (Wu et al.,

2018). Both strong hydrologic connectivity (α) and removal kinetics (λ , λ_I) are required for efficient nutrient removal (Bernhardt et al., 2017; Powers et al., 2012).

In the fall when vegetation decays, the sediment-water interface begins to play an equally important role in retention, particularly for particles (Figure 8). Most particles are likely deposited right at the sediment-water interface rather than being filtered along subsurface flow paths, given the fine texture of the streambed (Figure 5). Hyporheic exchange likely contributes little to no storage of solutes or particles below the sediment-water interface. This assumption is supported by the observation that the exchange rate coefficient (α) between mobile and immobile zones was greater in spring than fall by almost two orders of magnitude, but the concentration of particles captured in core samples was smaller by 65%. The commonly accepted mechanism for fine particle removal and retention in agricultural streams is deposition on the streambed (Hobbie and Likens, 1973; Hoffman et al., 2009), but this study suggests that vegetation can play an equal or greater role in all seasons. Earlier fine particle transport studies have focused on the role of particle storage in sediment (Cushing et al., 1993; Newbold et al., 2005; Paul and Hall Jr, 2002), but these studies were generally conducted in less modified streams, not dominated by heavy vegetation stands or characteristics of low gradient, intensely managed agricultural stream.

A decoupling was observed between SRP and particle transport, as indicated by the different uptake lengths across all seasons and the consistently larger kinetic rate constants for particle removal relative to SRP removal (Table 5). Earlier work has shown that particulate and organic matter bound P experiences shorter uptake lengths than soluble P (Newbold et al., 1983). This behavior also likely occurs during high flows because SRP can loosely bind to suspended sediment and may be released as in-stream conditions change (Dupas et al., 2015; King et al., 2022). It is possible that calculated particle uptake lengths (S_w , Table 3) approximate the uptake

lengths of particulate P over the timescale of tracer injection experiments. However, tracer injection experiments are not capable of resolving processes that act over longer timescales. Particulate P that is stored on vegetation or the streambed may be physically remobilized as particulate P during a high flow event, or as SRP if a change in chemical conditions allows desorption from particles (Casillas-Ituarte et al., 2019; Roden and Edmonds, 1997). Sediment bound P, particularly when associated with Fe-oxides, is more readily released under reducing conditions, which can occur in summer when decreases in flow coincide with warm water temperatures and declines in dissolved oxygen (Reddy et al., 1999; Simpson et al., 2021).

Despite the heavy modification of agricultural streams and often high SRP concentrations (Hoffman et al., 2009; Macrae et al., 2003), the stream studied here is an effective sink of P similar to natural headwater streams in the literature. When considering SRP, the uptake length in all seasons is within the range of values ($S_w = 15 - 506$ m) observed in earlier studies conducted in forested and urban landscapes (Famularo, 2019; Mulholland et al., 1990). Similarly, SRP uptake velocities also fall within the range of earlier observed values ($V_f = -1.7 - 53.5$ mm min⁻¹) in forested, agricultural, and urban landscapes (Ensign and Doyle, 2005; Famularo, 2019). This demonstrates that while these modified headwater streams are typically characterized by channel straightening and consolidated fine streambed materials that inhibit hyporheic exchange, vegetation can create substantial transient storage. Vegetation stands reduce velocity and promote solute and particle retention and also enhance morphologic complexity in the channel, forming pools and riffles and facilitates sedimentation over time (Blann et al., 2009; D'Ambrosio et al., 2015). This vegetation decomposes in the fall and can be washed out by high flow events in the winter and early spring, temporarily reducing storage capacity (Ensign and Doyle, 2005). This could be one of many factors that contribute to rising nutrient concentrations

in the Maumee River in the late winter, when vegetation has decayed, and declining concentrations in the spring, even while precipitation and runoff increase (Stow et al., 2015).

Not all agricultural streams and ditches have similar nutrient transport and transient storage characteristics. The size of the transient storage zone in this study was greater than in other studies of small agricultural streams (the proportional area of the transient storage zone, A_t/A , ranged from 0.21 – 0.53 at this site, compared to 0.10 – 0.30 in other studies) (Bernot et al., 2006; Sheibley et al., 2014). Factors that may control the development of transient storage are the age of the ditch, whether it develops mature submerged vegetation stands, and whether the ditch has a forested riparian buffer, which would influence aquatic vegetation growth. For example, the lower of transient storage values observed by Bernot et al. (2006) may be due to less intense aquatic vegetation (visual inspection of satellite data shows that some of these study reaches may be forested and therefore host less aquatic vegetation, while others are very straight with little vegetation in the stream channel, although stream characteristics may have changed between the study period and satellite imagery).

Limitations and Future Work

This study only examined solute and particle transport under moderate flow conditions in three seasons. For both P and fine particles, it can be expected that transport and retention characteristics will vary substantially over even shorter timescales like storm events, when significant amounts of P may be mobilized from adjacent croplands, the streambed, and vegetation (Bol et al., 2016; Harvey et al., 2012; Hobbie and Likens, 1973). During these events, vegetation may offer less resistance as it becomes fully submerged or bends under extreme flows. It has been shown that the export of P associated with fine particulate organic matter is greatly increased during high flow events in a unforest watershed relative to a forested

watershed (Hobbie and Likens, 1973). Moreover, agricultural headwater streams often exhibit flashy storm flow responses (Miller and Lyon, 2021). Thus, repeating these experiments during a high-flow event would help understand how remobilized P and fine particles are transported during the fastest export rates, when immobile storage zones may shrink and mobile zones may expand (Correll et al., 1999; Gao and Josefson, 2012).

This study also focuses on a reach where a two-stage ditch was installed for the purposes of increasing bank stability and decreasing nutrient and sediment export loads (Davis et al., 2015; Kallio et al., 2010; Mahl et al., 2015). The site now has a relatively stable channel with diverse pool and riffle features. Conversely, in newer or unrestored ditches that lack morphological and hydraulic diversity, straighter channels and more recently exposed sediment may have a differing impact on transport and retention dynamics. Thus, more studies are needed to capture the full range of hydrologic, ecologic, and biogeochemical conditions in agricultural drainage ditches.

Continued use of particle tracers in various stream sites and flow conditions will help elucidate fine particle transport behavior in agricultural streams. This study builds on previous fine particle transport studies from larger streams and more natural stream environments (Cushing et al., 1993; Minshall et al., 2000; Newbold et al., 2005; Paul and Hall, 2002). Harvey et al. (2012) showed that transient storage models could not describe fine particle transport as accurately as conservative solute transport, perhaps because particles may be subject to a greater range of velocities and variable mass transfer rates across different mobile and immobile compartments within streams than solutes (Drummond et al., 2014). Particle transport behavior has been more accurately described by mathematical models that can capture non-Gaussian transport behavior, including flexible continuous-time random walk mobile-immobile domain

approaches (Aubeneau et al., 2015; Drummond et al., 2014). This is especially true in agricultural drainage ditches, with their dense stands of aquatic vegetation that trap particles. Thus, future opportunities exist to examine particle tracer tests for agricultural headwater streams using alternative modeling approaches.

This study highlights the importance of considering differences in simultaneous transport of dissolved nutrients and fine particles that are often associated with sorbed nutrients (de Jonge et al., 2004). This work demonstrates that it is critical to continue evaluating how fine particle transport is coupled or decoupled from dissolved nutrient transport, particularly in the case of P. However, the co-injection of KH_2PO_4 and fluorescent particles presents several unique challenges. First, Dayglo particles are mildly hydrophobic and require the addition of a surfactant to aid mixing. I used SHMP, a phosphate salt, which contributed more dissolved P than KH_2PO_4 alone. The use of a phosphate-free dispersant would allow for nutrient uptake metric estimations at lower P concentrations, which would minimize impacts to stream biota and P uptake kinetics (Stream Solute Workshop, 1990). It has also been observed that SRP sorbs to Dayglo particles (Benefiel, 2022). The sorption behavior of SRP to both the particle tracer and natural sediments could be compared and incorporated in future transport models with further laboratory quantification. The SRP sorption affinity to Dayglo fine particles exhibited behavior seemingly sensitive to pH and other ambient conditions, as has been shown for SRP sorption affinity to natural sediments, and these sorption dynamics are beyond the scope of this study.

Conclusions

This novel study demonstrating the co-injection of dissolved P with a particle tracer highlights the key role of aquatic vegetation in nutrient and fine particle transport and retention in open-canopy agricultural headwater streams that lack shading from woody riparian vegetation.

By obstructing large portions of the channel, aquatic vegetation stands improve hydrologic complexity in otherwise morphologically simple channels. The resulting pools and riffles enhance exchange between the actively flowing mobile zone and the relatively immobile vegetation stand. This increased transient storage within a stream leads to longer residence times and more opportunity for biological nutrient uptake, particle capture, and biogeochemical transformation. Because vegetation growth is seasonal, with emergent vegetation being dense in the spring and then dying back in the summer and decaying in the fall, fine particle and SRP transport behavior responds seasonally. Specifically, I observed that the greatest particle retention and SRP uptake occurred in the spring, when dense emergent vegetation is dominant. This further supports a growing body of literature that demonstrates the impact of aquatic vegetation on the downstream transport of nutrients (Alnoee et al., 2021; Biggs et al., 2021; Greer et al., 2017).

Through the application of a novel tracer combination of fine particles and KH_2PO_4 , I quantified differences in the transport of SRP and fine particles (a tool for understanding particulate P) across seasons. Using similar tracer approaches in headwater streams with various management histories could provide more insight into drivers of nutrient transport and retention in large agricultural watersheds, like the Lake Erie Basin. Quantifying these transport behaviors is critical for guiding best management practices in small streams and understanding their impact on downstream water quality (Van Meter and Basu, 2017; Mohamed et al., 2019).

Tables

Table 1. Details of continuous spring (May), summer (July), and fall (December) stream injections. SRP is reported as phosphate as phosphorus (P-PO₄). Concentrations describe in-bucket injectate concentrations.

	Date of release		
	21 May 2021	07 July 2021	04 December 2021
Injection duration (min)	78	95	80
Injected volume (L)	55	39	40
Injectate Cl concentration (g/L)	143.0	146.3	167.1
Injectate P-PO ₄ concentration (mg/L)	0.52	1.20	0.83
Injectate Dayglo concentration (g/L)	8.0	48.6	32.7

Table 2. Average physical and chemical stream measurements during respective spring (May), summer (July), and fall (December) nutrient additions. May pH, oxidation-reduction potential, and dissolved oxygen measurements were made using an unfiltered 1-L water sample collected in the field and transport back to the lab on ice, while July and December water quality measurements were made in the field. b.d. = below detection (0.001 mg/L).

Parameter	Date of Release		
	21 May 2021*	22 July 2021	04 December 2021
Streamflow (L/s)	13.0	9.6	4.7
Water temp (°C)	13.1 – 18.3	19.0 – 28.6	3.8 – 7.4
Stream column pH	6.5	7.5	6.3
Stream column oxidation reduction potential (mV)	133.6	257.5	225.4
Stream column dissolved oxygen (mg/L)	9.16	6.64	8.24
Stream column SRP concentration (mg/L)	0.003	b.d.	0.003
Equilibrium phosphorus concentration in streambed cores (EPC ₀) (mg P/L)	0.012	0.002	0.012

Table 3. Nutrient and fine particle uptake and filtration metrics.

Parameter	Name	Unit	Spring		Summer		Fall	
			Phosphate	Particles	Phosphate	Particles	Phosphate	Particles
Storage area ratio	$A_I/(A + A_I)$	[]	0.35		0.18		0.19	
Spiraling length	$L_s = u/\alpha$	[m]	5.33		162.50		85.71	
Residence time in transient storage	$T_{sto} = A_I/\alpha A$	[sec]	53.33		1071.43		666.67	
Uptake length	$S_w = \frac{x}{\ln\left(\frac{C_{up}}{C_{down}}\right)}$	[m]	72.92	21.57	364.17	154.86	633.47	90.45
Uptake velocity	V_f	[mm/sec]	0.22	0.74	0.03	0.07	0.01	0.05

Table 4. Best fit parameters for OTIS simulations for conservative (Cl tracer) transport in the experimental reach observed during each season. Stream discharge (Q) was determined from plateau concentrations rather than model-data fitting and is only listed for reference.

Parameter	Unit	Season		
		Spring	Summer	Autumn
Q	[m ³ /sec]	0.024	0.0091	0.0045
Q_L	[m ³ /sec]	0.00	0.00	0.00
A	[m ²]	0.45	0.28	0.15
A_l	[m ²]	0.24	0.06	0.04
$u = Q/A$	[m/sec]	0.053	0.0325	0.03
D	[m ² /sec]	0.07	0.02	0.03
α	[/sec]	0.01	0.00020	0.00035

Table 5. Best fit parameters for nonconservative removal of SRP and fine particles.

Parameter	Unit	Season					
		Spring		Summer		Fall	
		SRP	Particles	SRP	Particles	SRP	Particles
λ	[/sec]	1.8×10^{-4}	1.4×10^{-3}	4.0×10^{-6}	4.0×10^{-4}	1.3×10^{-5}	2.0×10^{-4}
λ_I	[/sec]	1.8×10^{-4}	1.4×10^{-3}	4.0×10^{-6}	4.0×10^{-4}	1.3×10^{-5}	2.0×10^{-4}
$\hat{\lambda}$	[/sec]	2.5×10^{-5}	0.00	0.00	0.00	0.00	0.00
$\hat{\lambda}_I$	[/sec]	2.5×10^{-5}	0.00	0.00	0.00	0.00	0.00
ρ	[mg/m ³]	5.0×10^5	0.00	5.0×10^5	0.00	5.0×10^5	0.00
K_d	[m ³ /mg]	1.0×10^{-5}	0.00	1.0×10^{-5}	0.00	1.0×10^{-5}	0.00

Figures

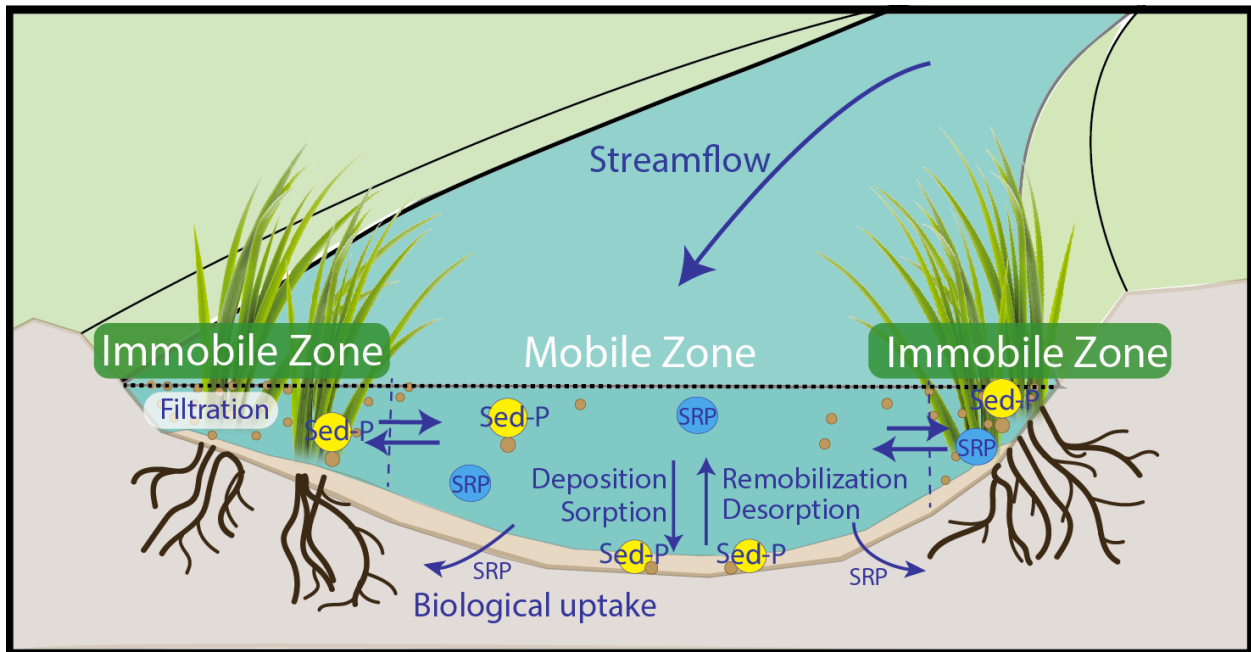


Figure 1. Conceptualization of processes affecting P transport in a stream with aquatic vegetation.

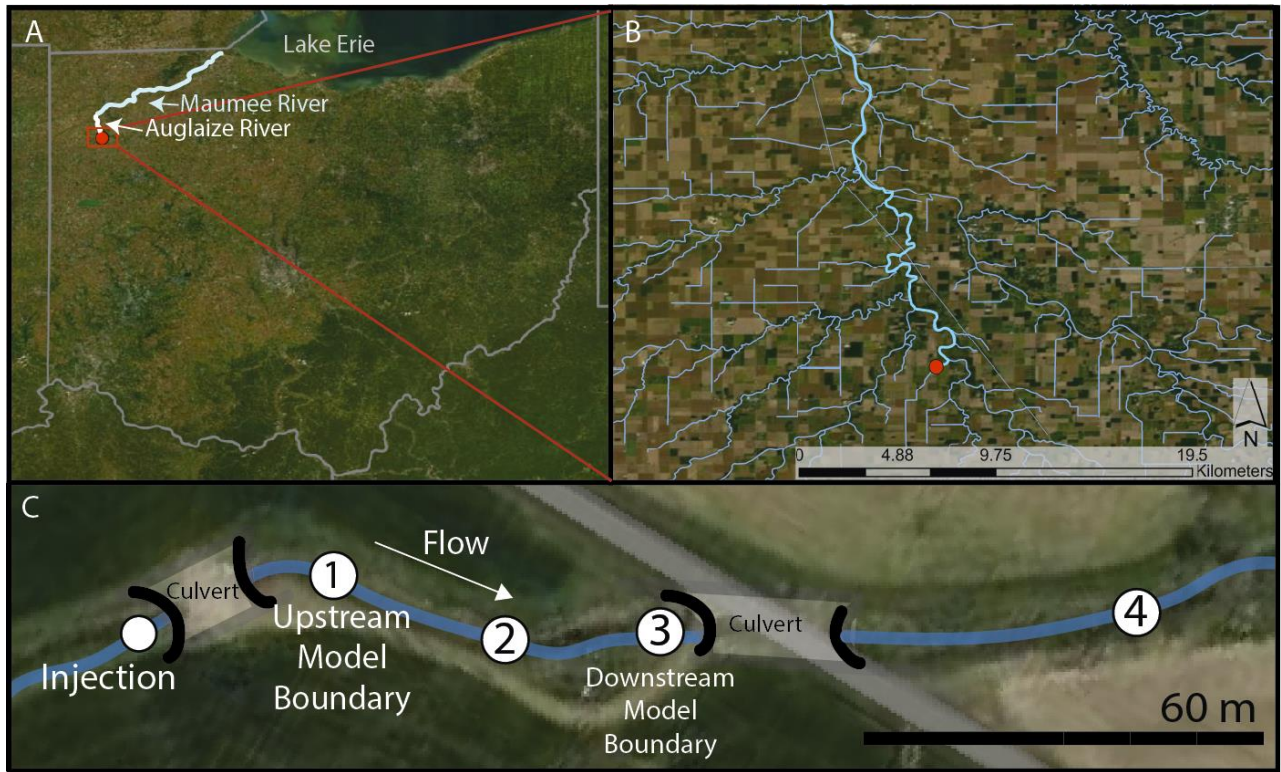


Figure 2. A) Flow path from study site to Lake Erie. B) Map of study site and nearby agricultural headwater streams and linear ditches C) Map of the experimental reach, injection location, and sampling stations. The model reach lies between station 1 and 3. Other stations were used only for dilution gauging and nutrient uptake estimates.

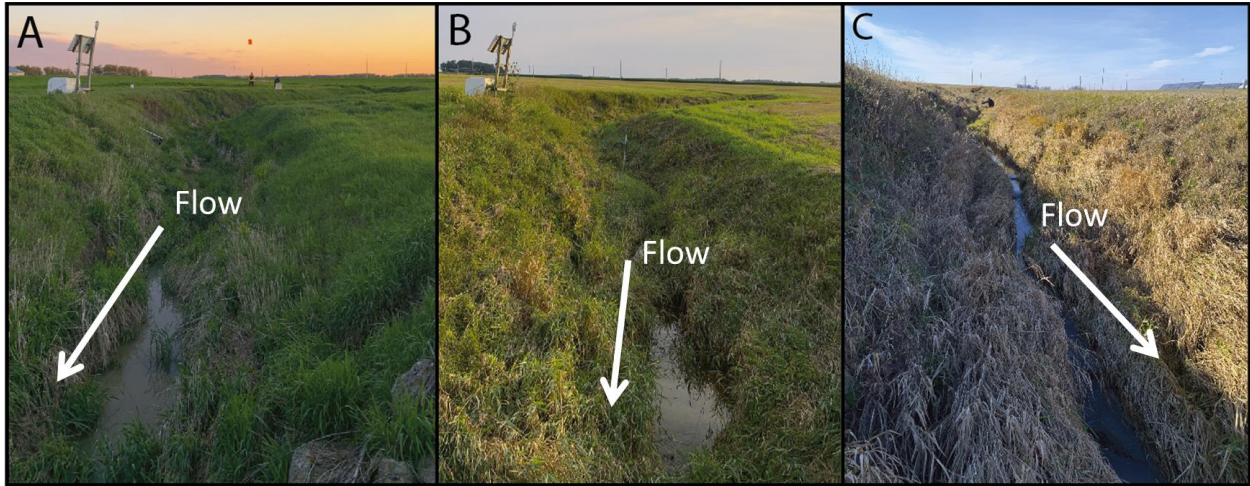


Figure 3. Stream site conditions in (A) May, (B) July, and (C) December, illustrating emergent vegetation stands in spring, mature vegetation in the summer, and the die off and decay of vegetation in the fall. Photos taken at station 3 in Figure 2C

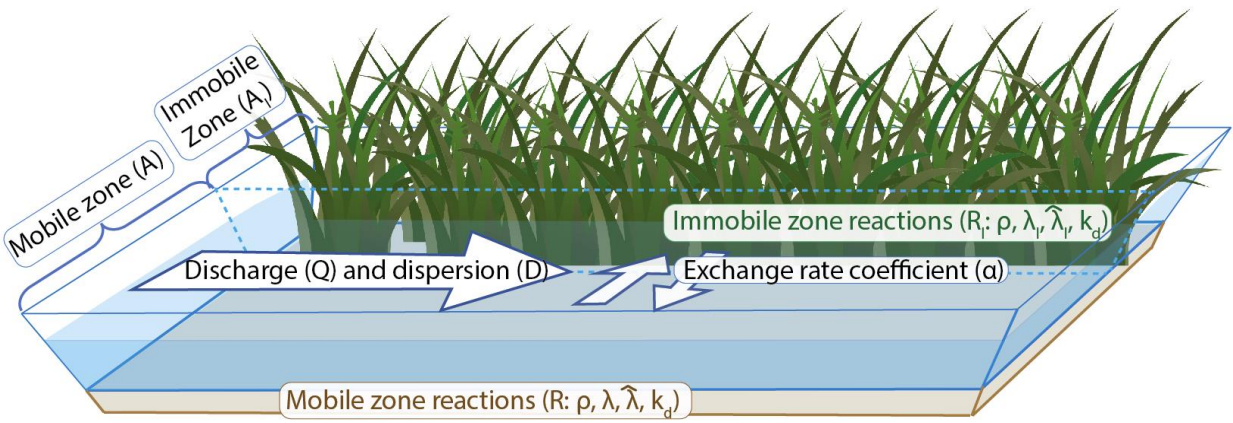


Figure 4. Schematic of compartments and processes incorporated in the OTIS model.

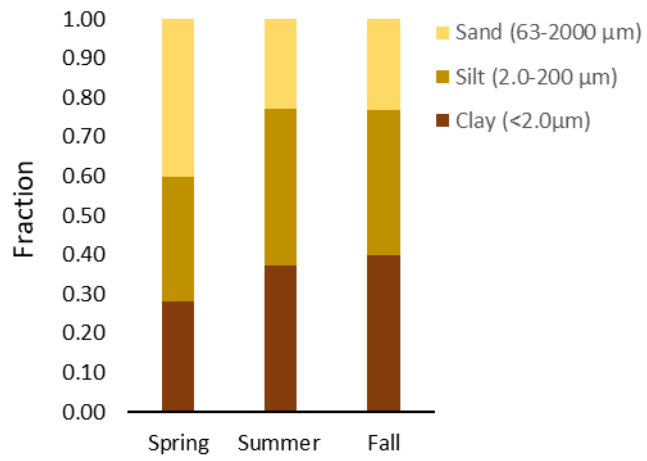


Figure 5. Particle size fractions of streambed sediment in each season.

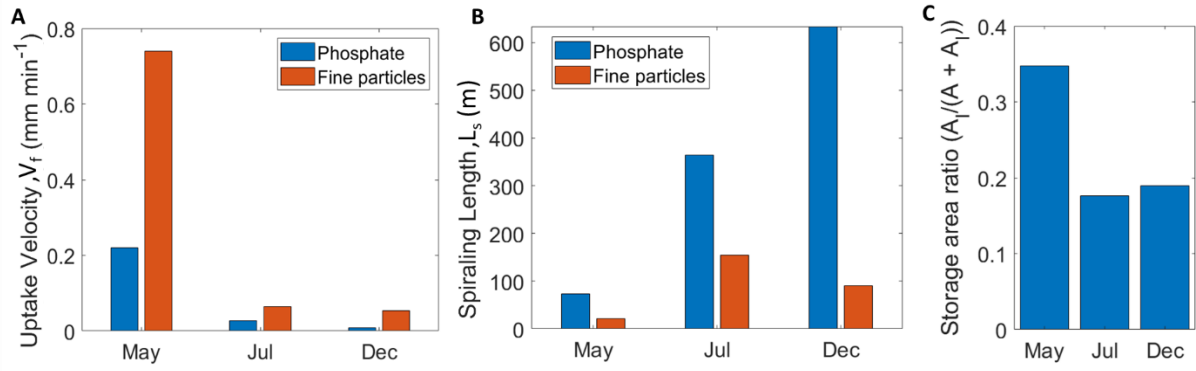


Figure 6. (A) SRP uptake velocity and fine particle uptake velocity, (B) spiraling lengths, and (C) storage area to total stream channel area fraction.

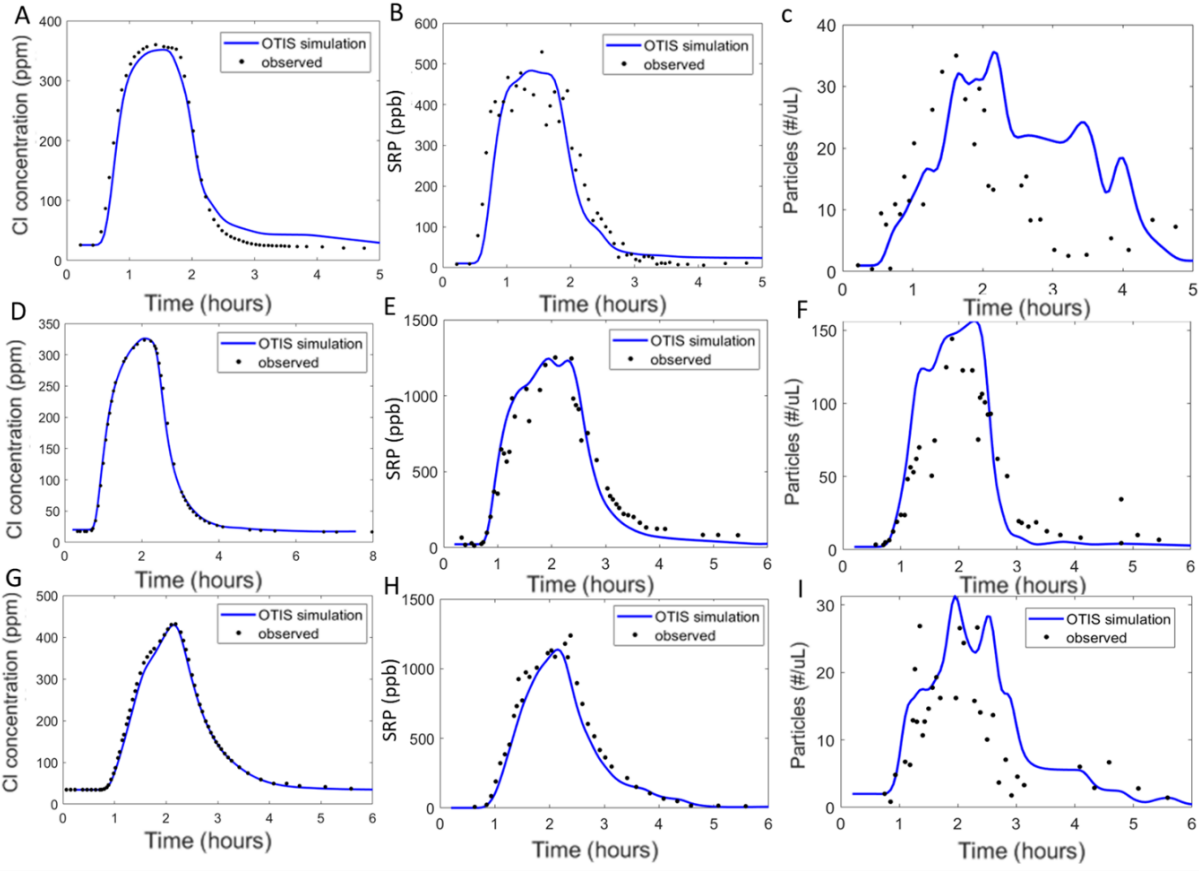


Figure 7. OTIS fits for Cl, P, and fine particles for the May injection (A-C), July injection (D-F), and December injection (G-I).

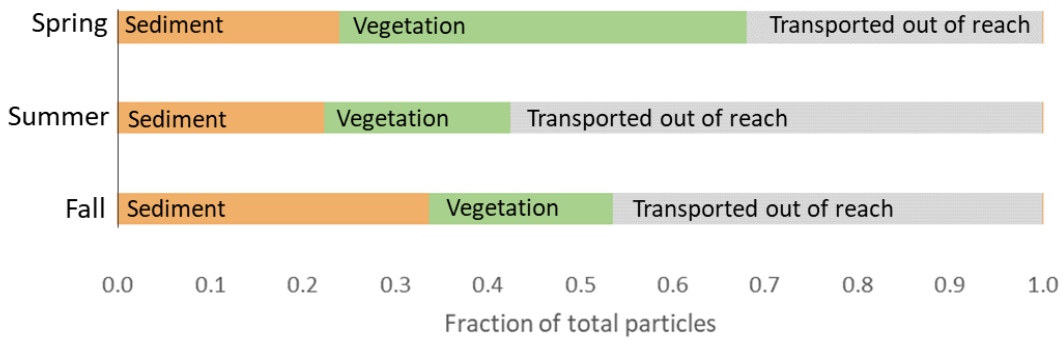


Figure 8. Estimated fraction of total particles retained in either the sediment or vegetation after each injection calculated from sediment and vegetation samples.

Bibliography

- Alnoee, A. B., Levi, P. S., Baattrup-Pedersen, A. and Riis, T.: Macrophytes enhance reach-scale metabolism on a daily, seasonal and annual basis in agricultural lowland streams, *Aquat. Sci.*, 83(1), 1–12, 2021.
- APHA: Standard methods for examination of water and wastewater, Am. Public Heal. Assoc., 9, 1998.
- Aubeneau, A. F., Drummond, J. D., Schumer, R., Bolster, D., Tank, J. L. and Packman, A. I.: Effects of benthic and hyporheic reactive transport on breakthrough curves, *Freshw. Sci.*, 34(1), 301–315, 2015.
- Baken, S., Moens, C., van der Grift, B. and Smolders, E.: Phosphate binding by natural iron-rich colloids in streams, *Water Res.*, 98, 326–333, 2016.
- Barko, J. W., Gunnison, D. and Carpenter, S. R.: Sediment interactions with submersed macrophyte growth and community dynamics, *Aquat. Bot.*, 41(1–3), 41–65, 1991.
- Basu, N. B., Destouni, G., Jawitz, J. W., Thompson, S. E., Loukinova, N. V, Darracq, A., Zanardo, S., Yaeger, M., Sivapalan, M. and Rinaldo, A.: Nutrient loads exported from managed catchments reveal emergent biogeochemical stationarity, *Geophys. Res. Lett.*, 37(23), 2010.
- Bencala, K. E. and Walters, R. A.: Simulation of solute transport in a mountain pool-and-riffle stream: A transient storage model, *Water Resour. Res.*, 19(3), 718–724, doi:10.1029/WR019i003p00718, 1983.
- Benefiel, R.: Batch Experiments to Understand Phosphorus and Fine Particle Interactions, The Ohio State University., 2022.
- Bernhardt, E. S., Blaszczak, J. R., Ficken, C. D., Fork, M. L., Kaiser, K. E. and Seybold, E. C.: Control points in ecosystems: moving beyond the hot spot hot moment concept, *Ecosystems*, 20(4), 665–682, 2017.
- Bernot, M. J., Tank, J. L., Royer, T. V and David, M. B.: Nutrient uptake in streams draining agricultural catchments of the midwestern United States, *Freshw. Biol.*, 51(3), 499–509, 2006.
- Biggs, H. J., Haddadchi, A. and Hicks, D. M.: Interactions between aquatic vegetation, hydraulics and fine sediment: A case study in the Halswell River, New Zealand, *Hydrol. Process.*, 35(6), e14245, 2021.
- Blann, K. L., Anderson, J. L., Sands, G. R. and Vondracek, B.: Effects of agricultural drainage on aquatic ecosystems: A review, *Crit. Rev. Environ. Sci. Technol.*, 39(11), 909–1001, doi:10.1080/10643380801977966, 2009.
- Bohrman, K. J. and Strauss, E. A.: Macrophyte-driven transient storage and phosphorus uptake in a western Wisconsin stream, *Hydrol. Process.*, 32(2), 253–263, 2018.
- Bol, R., Julich, D., Brödlin, D., Siemens, J., Kaiser, K., Dippold, M. A., Spielvogel, S., Zilla, T., Mewes, D. and von Blanckenburg, F.: Dissolved and colloidal phosphorus fluxes in forest ecosystems—an almost blind spot in ecosystem research, *J. Plant Nutr. Soil Sci.*, 179(4), 425–438, 2016.
- Brueske, C. C. and Barrett, G. W.: Effects of vegetation and hydrologic load on sedimentation patterns in experimental wetland ecosystems, *Ecol. Eng.*, 3(4), 429–447, 1994.
- Burrows, R. M., Fellman, J. B., Magierowski, R. H. and Barmuta, L. A.: Greater phosphorus uptake in forested headwater streams modified by clearfell forestry, *Hydrobiologia*, 703(1), 1–14, 2013.
- Capiesius, J. P., Sullivan, J. R., O’Neill, G. B. and Williams, C. A.: Using the tracer-dilution discharge method to develop streamflow records for ice-affected streams in Colorado, U. S.

Geological Survey., 2005.

Carignan, R.: An empirical model to estimate the relative importance of roots in phosphorus uptake by aquatic macrophytes, *Can. J. Fish. Aquat. Sci.*, 39(2), 243–247, 1982.

Casillas-Ituarte, N. N., Sawyer, A. H., Danner, K. M., King, K. W. and Covault, A. J.: Internal Phosphorus Storage in Two Headwater Agricultural Streams in the Lake Erie Basin, *Environ. Sci. Technol.*, doi:10.1021/acs.est.9b04232, 2019.

Correll, D. L., Jordan, T. E. and Weller, D. E.: Transport of nitrogen and phosphorus from Rhode River watersheds during storm events, *Water Resour. Res.*, 35(8), 2513–2521, 1999.

Cushing, C. E., Minshall, G. W. and Newbold, J. D.: Transport dynamics of fine particulate organic matter in two Idaho streams, *Limnol. Oceanogr.*, 38(6), 1101–1115, 1993.

D'Ambrosio, J. L., Ward, A. D. and Witter, J. D.: Evaluating Geomorphic Change in Constructed Two-Stage Ditches, *JAWRA J. Am. Water Resour. Assoc.*, 51(4), 910–922, 2015.

Davis, R. T., Tank, J. L., Mahl, U. H., Winikoff, S. G. and Roley, S. S.: The influence of two-stage ditches with constructed floodplains on water column nutrients and sediments in agricultural streams, *JAWRA J. Am. Water Resour. Assoc.*, 51(4), 941–955, 2015.

Drummond, J., Wright-Stow, A., Franklin, P., Quinn, J. and Packman, A.: Fine particle transport dynamics in response to wood additions in a small agricultural stream, *Hydrol. Process.*, 34(21), 4128–4138, doi:10.1002/hyp.13874, 2020.

Drummond, J. D., Davies-Colley, R. J., Stott, R., Sukias, J. P., Nagels, J. W., Sharp, A. and Packman, A. I.: Retention and remobilization dynamics of fine particles and microorganisms in pastoral streams, *Water Res.*, 66, 459–472, doi:10.1016/j.watres.2014.08.025, 2014.

Drummond, J. D., Larsen, L. G., González-Pinzón, R., Packman, A. I. and Harvey, J. W.: Fine particle retention within stream storage areas at base flow and in response to a storm event, *Water Resour. Res.*, 53(7), 5690–5705, doi:10.1002/2016WR020202, 2017.

Dupas, R., Gascuel-Oudou, C., Gilliet, N., Grimaldi, C. and Gruau, G.: Distinct export dynamics for dissolved and particulate phosphorus reveal independent transport mechanisms in an arable headwater catchment, *Hydrol. Process.*, 29(14), 3162–3178, 2015.

Durner, W. and Iden, S. C.: The improved integral suspension pressure method (ISP+) for precise particle size analysis of soil and sedimentary materials, *Soil Tillage Res.*, 213, 105086, 2021.

Ensign, S. H. and Doyle, M. W.: Ensign, Scott H., and Martin W. Doyle. In-channel transient storage and associated nutrient retention: Evidence from experimental manipulations. *Limnol. Oceanogr.*, 50(6), 2005, 1740–1751., 2005.

Famularo, J. T.: Nutrient Uptake Among Urban and Non-Urban Streams Within the Piedmont Physiographic Province of Virginia, 2019.

Fauria, K. E., Kerwin, R. E., Nover, D. and Schladow, S. G.: Suspended particle capture by synthetic vegetation in a laboratory flume, *Water Resour. Res.*, 51(11), 9112–9126, 2015.

Froelich, P. N.: Kinetic control of dissolved phosphate in natural rivers and estuaries: A primer on the phosphate buffer mechanism1, *Limnol. Oceanogr.*, 33(4part2), 649–668, doi:10.4319/lo.1988.33.4part2.0649, 1988.

Gao, P. and Josefson, M.: Temporal variations of suspended sediment transport in Oneida Creek watershed, central New York, *J. Hydrol.*, 426–427, 17–27, doi:https://doi.org/10.1016/j.jhydrol.2012.01.012, 2012.

Gebauer, A., Brown, R., Schwab, S., Mcneely, C. and Nezat, C.: Ecohydrology of invasive reed canary grass (*Phalaris arundinacea*), 2012.

Greer, M. J. C., Hicks, A. S., Crow, S. K. and Closs, G. P.: Effects of mechanical macrophyte

control on suspended sediment concentrations in streams, *New Zeal. J. Mar. Freshw. Res.*, 51(2), 254–278, 2017.

Harvey, J. W. and Wagnert, B. J.: *Zones Interactions between*, Elsevier Inc., 2000.

Harvey, J. W., Drummond, J. D., Martin, R. L., McPhillips, L. E., Packman, A. I., Jerolmack, D. J., Stonedahl, S. H., Aubeneau, A. F., Sawyer, A. H., Larsen, L. G. and Tobias, C. R.: Hydrogeomorphology of the hyporheic zone: Stream solute and fine particle interactions with a dynamic streambed, *J. Geophys. Res. Biogeosciences*, 117(4), 1–20, doi:10.1029/2012JG002043, 2012.

Hobbie, J. E. and Likens, G. E.: OUTPUT OF PHOSPHORUS, DISSOLVED ORGANIC CARBON, AND FINE PARTICULATE CARBON FROM HUBBARD BROOK WATERSHEDS 1, *Limnol. Oceanogr.*, 18(5), 734–742, 1973.

Hoffman, A. R., Armstrong, D. E., Lathrop, R. C. and Penn, M. R.: Characteristics and influence of phosphorus accumulated in the bed sediments of a stream located in an agricultural watershed, *Aquat. Geochemistry*, 15(3), 371–389, 2009.

Horton, R. E.: Erosional development of streams and their drainage basins; hydrophysical approach to quantitative morphology, *Geol. Soc. Am. Bull.*, 56(3), 275–370, 1945.

House, W. A., Jickells, T., Edwards, A. C., Praska, K. and Denison, F.: Reactions of phosphorus with sediments in fresh and marine waters, *Soil Use Manag.*, 14, 139–146, doi:10.1111/j.1475-2743.1998.tb00632.x, 2007.

Huang, Y. H., Saiers, J. E., Harvey, J. W., Noe, G. B. and Mylon, S.: Advection, dispersion, and filtration of fine particles within emergent vegetation of the Florida Everglades, *Water Resour. Res.*, 44(4), 2008.

Jankowiak, J., Hattenrath-Lehmann, T., Kramer, B. J., Ladds, M. and Gobler, C. J.: Deciphering the effects of nitrogen, phosphorus, and temperature on cyanobacterial bloom intensification, diversity, and toxicity in western Lake Erie, *Limnol. Oceanogr.*, 64(3), 1347–1370, 2019.

de Jonge, L. W., Moldrup, P., Rubæk, G. H., Schelde, K. and Djurhuus, J.: Particle Leaching and Particle-Facilitated Transport of Phosphorus at Field Scale, *Vadose Zo. J.*, 3(2), 462–470, doi:10.2136/vzj2004.0462, 2004.

Kallio, R., Ward, A., D’Ambrosio, J. and Witter, J. D.: A decade later: the establishment, channel evolution, and stability of innovative two-stage agricultural ditches in the midwest region of the United States, in 9th International Drainage Symposium held jointly with CIGR and CSBE/SCGAB Proceedings, 13-16 June 2010, Québec City Convention Centre, Québec City, Canada, p. 1, American Society of Agricultural and Biological Engineers., 2010.

Kincaid, D. W., Seybold, E. C., Adair, E. C., Bowden, W. B., Perdrial, J. N., Vaughan, M. C. H. and Schroth, A. W.: Land use and season influence event-scale nitrate and soluble reactive phosphorus exports and export stoichiometry from headwater catchments, *Water Resour. Res.*, 56(10), e2020WR027361, 2020.

King, K. W., Fausey, N. R. and Williams, M. R.: Effect of subsurface drainage on streamflow in an agricultural headwater watershed, *J. Hydrol.*, 519, 438–445, 2014.

King, W. M., Curless, S. E. and Hood, J. M.: River phosphorus cycling during high flow may constrain Lake Erie cyanobacteria blooms, *Water Res.*, 118845, 2022.

Ky, N. M., Hung, N. T. Q., Manh, N. C., Lap, B. Q., Dang, H. T. T. and Ozaki, A.: Assessment of nutrients removal by constructed wetlands using Reed Grass (*Phragmites australis* L.) and Vetiver Grass (*Vetiveria Zizanioides* L.), 2020.

Macrae, M. L., English, M. C., Schiff, S. L. and Stone, M. A.: Phosphate retention in an agricultural stream using experimental additions of phosphate, *Water Resour. Res.*, 36(6), 3663–3666, 2000.

doi:10.1002/hyp.1356, 2003.

Mahl, U. H., Tank, J. L., Roley, S. S. and Davis, R. T.: Two-stage ditch floodplains enhance N-removal capacity and reduce turbidity and dissolved P in agricultural streams, *JAWRA J. Am. Water Resour. Assoc.*, 51(4), 923–940, 2015.

McCorvie, M. R. and Lant, C. L.: Drainage district formation and the loss of Midwestern wetlands, 1850-1930, *Agric. Hist.*, 67(4), 13–39, 1993.

Van Meter, K. J. and Basu, N. B.: Time lags in watershed-scale nutrient transport: an exploration of dominant controls, *Environ. Res. Lett.*, 12(8), 84017, 2017.

Miller, S. A. and Lyon, S. W.: Tile drainage causes flashy streamflow response in Ohio watersheds, *Hydrol. Process.*, 35(8), e14326, 2021.

Minshall, G. W., Thomas, S. A., Newbold, J. D., Monaghan, M. T. and Cushing, C. E.: Physical factors influencing fine organic particle transport and deposition in streams, *J. North Am. Benthol. Soc.*, 19(1), 1–16, 2000.

Mohamed, M. N., Wellen, C., Parsons, C. T., Taylor, W. D., Arhonditsis, G., Chomicki, K. M., Boyd, D., Weidman, P., Mundle, S. O. C. and Cappellen, P. Van: Understanding and managing the re-eutrophication of Lake Erie: Knowledge gaps and research priorities, *Freshw. Sci.*, 38(4), 675–691, 2019.

Mulholland, P. J., Steinman, A. D. and Elwood, J. W.: Measurement of phosphorus uptake length in streams: comparison of radiotracer and stable PO₄ releases, *Can. J. Fish. Aquat. Sci.*, 47(12), 2351–2357, doi:10.1139/f90-261, 1990.

Myers, D. N., Metzker, K. D. and Davis, S.: Status and trends in suspended-sediment discharges, soil erosion, and conservation tillage in the Maumee River basin--Ohio, Michigan, and Indiana, US Department of the Interior, US Geological Survey., 2000.

Nadeau, T. and Rains, M. C.: Hydrological connectivity between headwater streams and downstream waters: how science can inform policy 1, *JAWRA J. Am. Water Resour. Assoc.*, 43(1), 118–133, 2007.

Needelman, B. A., Kleinman, P. J. A., Strock, J. S. and Allen, A. L.: Drainage Ditches: Improved management of agricultural drainage ditches for water quality protection: An overview, *J. Soil Water Conserv.*, 62(4), 171–178, 2007.

Nepf, H. M.: Flow and transport in regions with aquatic vegetation, 2012.

Newbold, J. D., Elwood, J. W., O’neill, R. V and Sheldon, A. L.: Phosphorus dynamics in a woodland stream ecosystem: a study of nutrient spiralling, *Ecology*, 64(5), 1249–1265, 1983.

Newbold, J. D., Thomas, S. A., Minshall, G. W., Cushing, C. E. and Georgian, T.: Deposition, benthic residence, and resuspension of fine organic particles in a mountain stream, *Limnol. Oceanogr.*, 50(5), 1571–1580, 2005.

O’Brien, J. M., Lessard, J. L., Plew, D., Graham, S. E. and McIntosh, A. R.: Aquatic macrophytes alter metabolism and nutrient cycling in lowland streams, *Ecosystems*, 17(3), 405–417, 2014.

Paul, M. J. and Hall Jr, R. O.: Particle transport and transient storage along a stream-size gradient in the Hubbard Brook Experimental Forest, *J. North Am. Benthol. Soc.*, 21(2), 195–205, 2002.

Powers, S. M., Stanley, E. H. and Lottig, N. R.: Quantifying phosphorus uptake using pulse and steady-state approaches in streams, *Limnol. Oceanogr. Methods*, 7(7), 498–508, 2009.

Powers, S. M., Johnson, R. A. and Stanley, E. H.: Nutrient retention and the problem of hydrologic disconnection in streams and wetlands, *Ecosystems*, 15(3), 435–449, 2012.

Rabalais, N. N. and Turner, R. E.: Gulf of Mexico hypoxia: Past, present, and future, *Limnol. Oceanogr. Bull.*, 28(4), 117–124, 2019.

Reddy, K. R., Kadlec, R. H., Flaig, E. and Gale, P. M.: Streams and Wetlands: A Review, *Crit. Rev. Environ. Sci. Technol.*, 29(1), 83–146, doi:10.1080/10643389991259182, 1999.

Robertson, G. P., Coleman, D. C., Sollins, P. and Bledsoe, C. S.: Standard soil methods for long-term ecological research, Oxford University Press on Demand., 1999.

Roden, E. E. and Edmonds, J. W.: Phosphate mobilization in iron-rich anaerobic sediments: microbial Fe (III) oxide reduction versus iron-sulfide formation, *Arch. für Hydrobiol.*, 347–378, 1997.

Runkel, R. L.: One-dimensional transport with inflow and storage (otis): a solute transport model for streams and rivers, *Water-Resources Investig. Rep. 98-4018*, (January 1991), 0–80, doi:Cited By (since 1996) 47\nExport Date 4 April 2012, 1998.

Runkel, R. L., States, U. and Survey, G.: OTIS - (One-Dimensional Transport with Inflow and Storage: A Solute Transport Model for Streams and Rivers), *Encycl. Hydrol. Sci.*, (December), doi:10.1002/0470848944.hsa266, 2005.

Saiers, J. E., Harvey, J. W. and Mylon, S. E.: Surface-water transport of suspended matter through wetland vegetation of the Florida everglades, *Geophys. Res. Lett.*, 30(19), 2003.

Schilling, K. E. and Helmers, M.: Tile drainage as karst: Conduit flow and diffuse flow in a tile-drained watershed, *J. Hydrol.*, 349(3), 291–301, doi:https://doi.org/10.1016/j.jhydrol.2007.11.014, 2008.

Sheibley, R. W., Duff, J. H. and Tesoriero, A. J.: Low transient storage and uptake efficiencies in seven agricultural streams: Implications for nutrient demand, *J. Environ. Qual.*, 43(6), 1980–1990, 2014.

Simpson, Z. P., McDowell, R. W., Condron, L. M., McDaniel, M. D., Jarvie, H. P. and Abell, J. M.: Sediment phosphorus buffering in streams at baseflow: A meta-analysis, *J. Environ. Qual.*, 50(2), 287–311, 2021.

Smith, D. R.: Assessment of in-stream phosphorus dynamics in agricultural drainage ditches, *Sci. Total Environ.*, 407(12), 3883–3889, 2009.

Smith, D. R., Wilson, R. S., King, K. W., Zwonitzer, M., McGrath, J. M., Harmel, R. D., Haney, R. L. and Johnson, L. T.: Lake Erie, phosphorus, and microcystin: Is it really the farmer’s fault?, *J. Soil Water Conserv.*, 73(1), 48–57, 2018.

Stow, C. A., Cha, Y., Johnson, L. T., Confesor, R. and Richards, R. P.: Long-term and seasonal trend decomposition of Maumee River nutrient inputs to western Lake Erie, *Environ. Sci. Technol.*, 49(6), 3392–3400, 2015.

Sweeney, B. W. and Newbold, J. D.: Streamside forest buffer width needed to protect stream water quality, habitat, and organisms: a literature review, *JAWRA J. Am. Water Resour. Assoc.*, 50(3), 560–584, 2014.

Trentman, M. T., Dodds, W. K., Fencl, J. S., Gerber, K., Guarneri, J., Hitchman, S. M., Peterson, Z. and Rüegg, J.: Quantifying ambient nitrogen uptake and functional relationships of uptake versus concentration in streams: a comparison of stable isotope, pulse, and plateau approaches, *Biogeochemistry*, 125(1), 65–79, 2015.

Trentman, M. T., Tank, J. L., Jones, S. E., McMillan, S. K. and Royer, T. V: Seasonal evaluation of biotic and abiotic factors suggests phosphorus retention in constructed floodplains in three agricultural streams, *Sci. Total Environ.*, 729, 138744, 2020.

Vaughan, R. E., Needelman, B. A., Kleinman, P. J. A. and Allen, A. L.: Spatial Variation of Soil Phosphorus within a Drainage Ditch Network, *J. Environ. Qual.*, 36(4), 1096–1104, doi:10.2134/jeq2006.0095, 2007.

Weigelhofer, G.: The potential of agricultural headwater streams to retain soluble reactive

phosphorus, *Hydrobiologia*, 793(1), 149–160, doi:10.1007/s10750-016-2789-4, 2017.

Williams, M. R., King, K. W., Ford, W. and Fausey, N. R.: Edge-of-field research to quantify the impacts of agricultural practices on water quality in Ohio, *J. Soil Water Conserv.*, 71(1), 9A-12A, 2016.

Workshop, S. S.: Concepts and methods for assessing solute dynamics in stream ecosystems, *J. North Am. Benthol. Soc.*, 9(2), 95–119, 1990.

Wu, L., Gao, B. and Muñoz-Carpena, R.: Experimental analysis of colloid capture by a cylindrical collector in laminar overland flow, *Environ. Sci. Technol.*, 45(18), 7777–7784, 2011.

Wu, L., Gao, B., Muñoz-Carpena, R. and Pachepsky, Y. A.: Single collector attachment efficiency of colloid capture by a cylindrical collector in laminar overland flow, *Environ. Sci. Technol.*, 46(16), 8878–8886, 2012.

Wu, L., Munoz-Carpena, R., Gao, B., Yang, W. and Pachepsky, Y. A.: Colloid filtration in surface dense vegetation: Experimental results and theoretical predictions, *Environ. Sci. Technol.*, 48(7), 3883–3890, 2014.

Wu, Y., Liu, J. and Rene, E. R.: Periphytic biofilms: a promising nutrient utilization regulator in wetlands, *Bioresour. Technol.*, 248, 44–48, 2018.

Yu, C., Duan, P., Barry, D. A., Johnson, W. P., Chen, L., Yu, Z., Sun, Y. and Li, Y.: Colloidal transport and deposition through dense vegetation, *Chemosphere*, 287, 132197, 2022.

Appendix A. Solute and fine particle concentrations observed at the upstream sampling station (26 m) during the May injection experiment

Distance Downstream (m)	Time	Observed Cl (ppm)	Phosphate (ppb)	Particles (#/uL)
26	12:05:00 PM	25.94	13.10	n.d.
26	12:10:00 PM	n.d.	10.32	3.49
26	12:12:00 PM	n.d.	11.43	3.94
26	12:14:00 PM	n.d.	1.04	n.d.
26	12:16:00 PM	n.d.	22.46	4.99
26	12:18:00 PM	28.57	18.67	8.08
26	12:20:00 PM	42.35	47.90	9.80
26	12:22:00 PM	n.d.	186.92	15.00
26	12:25:00 PM	180.01	339.91	29.73
26	12:29:00 PM	n.d.	531.26	113.05
26	12:33:00 PM	316.09	628.54	80.93
26	12:37:00 PM	349.11	698.59	86.38
26	12:41:00 PM	355.11	711.31	87.01
26	12:45:00 PM	360.14	732.38	143.42
26	12:49:00 PM	n.d.	718.26	n.d.
26	12:53:00 PM	n.d.	664.84	151.04
26	12:57:00 PM	384.54	757.94	163.03
26	1:01:00 PM	n.d.	790.06	271.49
26	1:05:00 PM	n.d.	731.77	80.46
26	1:09:00 PM	299.88	737.17	159.36
26	1:13:00 PM	n.d.	716.84	n.d.
26	1:25:00 PM	383.59	728.94	414.85
26	1:29:00 PM	n.d.	678.45	359.55
26	1:31:00 PM	290.46	733.04	n.d.
26	1:35:00 PM	323.88	365.34	226.15
26	1:37:00 PM	n.d.	448.58	366.04
26	1:39:00 PM	n.d.	342.58	290.63
26	1:41:00 PM	n.d.	298.64	n.d.
26	1:44:00 PM	181.04	243.86	473.82
26	1:46:00 PM	n.d.	212.21	238.14
26	1:48:00 PM	159.09	192.75	217.18
26	1:51:00 PM	n.d.	151.32	330.89
26	1:53:00 PM	n.d.	126.75	428.55
26	1:55:00 PM	76.10	136.21	494.81
26	1:57:00 PM	119.05	128.68	347.77
26	1:59:00 PM	106.82	111.16	486.86
26	2:07:00 PM	63.44	120.93	172.49
26	2:17:00 PM	56.52	29.79	240.15
26	2:48:00 PM	40.96	13.87	n.d.
26	2:58:00 PM	28.38	15.75	216.05
26	3:13:00 PM	0.00	13.12	282.69
26	3:23:00 PM	n.d.	10.14	202.80
26	3:33:00 PM	41.81	10.25	53.51
26	3:43:00 PM	n.d.	n.d.	266.99
26	3:58:00 PM	17.14	10.37	71.69
26	4:33:00 PM	n.d.	11.19	10.52
26	5:03:00 PM	23.73	10.37	13.82
26	5:33:00 PM	n.d.	7.94	n.d.
26	5:53:00 PM	27.64	10.37	16.55
26	6:09:00 PM	n.d.	7.13	3.57
26	6:40:00 PM	n.d.	7.54	1.51
26	7:10:00 PM	n.d.	6.73	9.96

Appendix B. Solute and fine particle concentrations observed at the downstream sampling station (92 m) during the May injection experiment

Distance Downstream (m)	Time	Observed Cl (ppm)	Phosphate (ppb)	Particles (#/uL)
92	12:07:00 PM	26.14	7.65	n.d.
92	12:23:00 PM	25.80	8.34	1.01
92	12:35:00 PM	25.55	9.05	0.41
92	12:43:00 PM	47.80	78.52	9.43
92	12:47:00 PM	86.66	155.34	7.60
92	12:51:00 PM	138.43	281.93	0.48
92	12:55:00 PM	196.08	383.08	10.90
92	12:59:00 PM	250.30	407.07	9.29
92	1:03:00 PM	284.62	373.72	15.37
92	1:07:00 PM	308.54	407.03	11.46
92	1:11:00 PM	327.92	466.69	20.79
92	1:15:00 PM	340.11	385.07	n.d.
92	1:19:00 PM	347.19	446.00	10.88
92	1:23:00 PM	353.16	477.44	n.d.
92	1:27:00 PM	356.60	437.58	26.21
92	1:35:00 PM	360.13	424.02	32.38
92	1:43:00 PM	356.91	529.25	n.d.
92	1:47:00 PM	355.49	350.05	34.99
92	1:51:00 PM	354.86	396.78	n.d.
92	1:55:00 PM	352.65	431.20	27.91
92	1:59:00 PM	338.94	358.58	n.d.
92	2:03:00 PM	307.58	415.09	20.63
92	2:07:00 PM	264.09	433.95	29.62
92	2:11:00 PM	216.21	292.89	26.13
92	2:15:00 PM	172.87	239.46	13.88
92	2:19:00 PM	134.28	276.28	13.26
92	2:23:00 PM	106.15	202.74	n.d.
92	2:27:00 PM	84.23	167.43	n.d.
92	2:31:00 PM	68.21	115.68	n.d.
92	2:35:00 PM	57.73	133.78	n.d.
92	2:39:00 PM	49.74	119.64	n.d.
92	2:43:00 PM	43.93	100.36	13.94
92	2:47:00 PM	39.73	87.30	15.40
92	2:51:00 PM	36.78	59.01	8.29
92	2:55:00 PM	34.37	25.57	n.d.
92	2:59:00 PM	31.52	58.94	8.43
92	3:03:00 PM	29.53	30.86	n.d.
92	3:07:00 PM	27.86	32.73	n.d.
92	3:11:00 PM	26.58	20.15	3.51
92	3:15:00 PM	25.78	16.54	n.d.
92	3:19:00 PM	25.02	26.75	n.d.
92	3:23:00 PM	25.00	27.56	2.54
92	3:27:00 PM	24.65	23.95	n.d.
92	3:31:00 PM	24.26	8.53	n.d.
92	3:35:00 PM	24.40	11.21	n.d.
92	3:39:00 PM	24.00	10.21	2.71
92	3:43:00 PM	23.60	12.80	n.d.
92	3:51:00 PM	23.16	7.22	n.d.
92	4:00:00 PM	23.13	8.18	5.38
92	4:15:00 PM	22.61	5.89	3.50
92	4:35:00 PM	20.73	10.25	8.37
92	4:55:00 PM	20.42	11.10	7.26
92	5:15:00 PM	20.57	7.98	0.75
92	5:45:00 PM	19.76	5.84	4.68
92	6:25:00 PM	22.03	3.00	0.59
92	6:55:00 PM	22.64	3.18	0.93
92	7:23:00 PM	23.64	5.03	0.19

Appendix C. Solute and fine particle concentrations observed at the upstream sampling station
(26 m) during the July injection experiment

Distance Downstream (m)	Time	Observed Cl (ppm)	Phosphate (ppb)	Particles (#/uL)
26	10:49:00 AM	7.45	21.67	2.60
26	10:53:00 AM	7.73	12.60	2.58
26	11:01:00 AM	13.43	25.46	n.d.
26	11:03:00 AM	37.54	128.30	9.39
26	11:05:00 AM	74.98	299.59	16.45
26	11:06:00 AM	94.65	351.60	n.d.
26	11:07:00 AM	109.76	482.46	n.d.
26	11:08:00 AM	125.29	580.56	47.87
26	11:10:00 AM	149.59	667.69	59.71
26	11:15:00 AM	200.57	880.66	64.94
26	11:20:00 AM	248.16	1010.27	131.13
26	11:21:00 AM	n.d.	n.d.	99.19
26	11:23:00 AM	n.d.	n.d.	170.04
26	11:24:00 AM	268.01	1141.82	227.77
26	11:28:00 AM	284.54	1089.11	267.95
26	11:25:00 AM	n.d.	n.d.	283.03
26	11:34:00 AM	299.58	1194.45	247.79
26	11:47:00 AM	318.23	1151.11	236.47
26	11:55:00 AM	328.05	1264.20	290.32
26	12:10:00 PM	338.31	1389.90	293.10
26	12:19:00 PM	333.36	1197.17	n.d.
26	12:31:00 PM	321.76	1349.49	316.08
26	12:34:00 PM	318.70	1383.82	n.d.
26	12:36:00 PM	306.77	1188.82	304.39
26	12:38:00 PM	280.77	1259.59	314.37
26	12:51:00 PM	125.84	593.75	54.05
26	12:56:00 PM	91.05	417.91	71.49
26	1:00:00 PM	72.28	378.60	31.97
26	1:05:00 PM	59.53	251.03	15.85
26	1:14:00 PM	38.63	195.95	18.17
26	1:30:00 PM	24.72	127.80	4.76
26	1:45:00 PM	16.59	93.02	n.d.
26	2:00:00 PM	12.29	70.81	10.05
26	2:30:00 PM	8.10	55.93	5.66
26	3:00:00 PM	8.11	45.33	7.04
26	4:00:00 PM	5.85	21.49	n.d.
26	5:00:00 PM	4.67	37.41	2.83
26	6:00:00 PM	4.92	38.22	8.26
26	6:30:00 PM	4.63	37.91	2.32

Appendix D. Solute and fine particle concentrations observed at the downstream sampling station (92 m) during the July injection experiment

Distance Downstream (m)	Time	Observed Cl (ppm)	Phosphate (ppb)	Particles (#/uL)
92	11:05:00 AM	7.40	65.33	n.d.
92	11:09:00 AM	7.36	18.30	n.d.
92	11:16:00 AM	7.36	28.05	n.d.
92	11:19:00 AM	7.32	12.26	3.44
92	11:27:00 AM	8.82	24.10	3.27
92	11:29:00 AM	11.99	35.40	5.04
92	11:33:00 AM	24.47	97.52	6.51
92	11:37:00 AM	48.14	202.39	12.42
92	11:41:00 AM	80.55	367.79	19.03
92	11:45:00 AM	116.32	354.93	23.81
92	11:49:00 AM	153.72	646.14	23.67
92	11:52:00 AM	178.77	619.70	48.25
92	11:55:00 AM	196.50	566.21	56.32
92	11:58:00 AM	215.69	630.04	53.02
92	12:01:00 PM	232.12	982.57	62.11
92	12:04:00 PM	245.45	862.66	69.95
92	12:17:00 PM	279.35	1044.07	50.53
92	12:20:00 PM	284.53	832.77	74.65
92	12:32:00 PM	301.17	1037.47	124.77
92	12:38:00 PM	306.79	1202.10	144.18
92	12:49:00 PM	313.36	1251.50	122.64
92	12:59:00 PM	311.96	n.d.	122.63
92	1:05:00 PM	304.06	n.d.	75.32
92	1:07:00 PM	299.77	1245.04	104.01
92	1:09:00 PM	292.23	980.95	106.53
92	1:12:00 PM	276.50	937.83	100.77
92	1:15:00 PM	256.71	911.50	92.41
92	1:18:00 PM	236.39	705.40	92.91
92	1:25:00 PM	180.36	753.74	62.10
92	1:35:00 PM	115.34	575.99	50.34
92	1:47:00 PM	70.33	389.53	19.49
92	1:50:00 PM	63.14	339.33	18.38
92	1:53:00 PM	56.97	317.29	n.d.
92	1:57:00 PM	49.68	285.43	15.80
92	2:00:00 PM	44.50	260.89	n.d.
92	2:05:00 PM	38.78	221.60	18.72
92	2:10:00 PM	33.10	213.28	n.d.
92	2:16:00 PM	28.73	201.46	12.63
92	2:23:00 PM	24.27	163.53	n.d.
92	2:30:00 PM	20.78	132.27	10.07
92	2:42:00 PM	17.02	123.89	n.d.
92	2:51:00 PM	14.65	122.56	8.21
92	3:33:00 PM	9.82	83.46	4.49
92	3:50:00 PM	9.01	83.16	10.00
92	4:12:00 PM	8.12	81.27	6.76
92	5:28:00 PM	6.73	71.12	8.41
92	5:48:00 PM	6.41	52.10	5.86
92	6:43:00 PM	6.66	65.67	6.98

Appendix E. Solute and fine particle concentrations observed at the upstream sampling station
(26 m) during the December injection experiment

Distance Downstream (m)	Time (sec)	Observed Cl (ppm)	Phosphate (ppb)	Particles (#/uL)
26	0	34.38	n.d.	n.d.
26	240	34.34	n.d.	n.d.
26	420	34.37	n.d.	n.d.
26	600	34.32	0.84	3.28
26	780	34.27	n.d.	n.d.
26	960	34.34	7.01	2.70
26	1140	41.28	60.09	4.46
26	1320	82.76	186.80	12.08
26	1500	128.22	n.d.	n.d.
26	1680	168.82	n.d.	18.54
26	1860	179.51	493.23	50.16
26	2040	202.25	n.d.	n.d.
26	2220	236.16	599.77	16.26
26	2400	263.24	n.d.	n.d.
26	2580	294.90	804.67	31.34
26	2760	304.07	n.d.	n.d.
26	2940	336.35	831.86	51.08
26	3120	369.47	982.13	9.08
26	3300	378.38	1058.20	27.54
26	3480	406.45	n.d.	30.96
26	3660	395.80	n.d.	n.d.
26	3840	381.07	1078.47	39.35
26	4020	378.82	n.d.	n.d.
26	4200	388.55	1228.68	28.52
26	4380	404.88	n.d.	n.d.
26	4560	418.27	1176.84	67.05
26	4740	430.35	n.d.	n.d.
26	4920	441.60	1209.70	68.93
26	5100	459.25	n.d.	n.d.
26	5280	461.91	1289.95	22.89
26	5460	459.20	n.d.	n.d.
26	5640	487.02	1367.06	43.04
26	5820	447.95	1256.08	n.d.
26	6000	403.75	1107.04	22.89
26	6180	347.95	976.96	43.04
26	6360	291.16	848.90	32.25
26	6540	250.35	469.73	n.d.
26	6720	230.58	525.80	59.17
26	6900	202.62	n.d.	n.d.
26	7080	187.68	371.78	n.d.
26	7260	172.77	n.d.	n.d.
26	7440	155.04	n.d.	10.27
26	7620	144.05	n.d.	n.d.
26	7800	135.14	333.82	13.05
26	7980	127.04	n.d.	n.d.
26	8160	117.18	196.49	44.19
26	8340	114.40	n.d.	n.d.
26	8580	103.43	226.27	5.72
26	8820	95.86	n.d.	n.d.
26	9060	90.30	136.29	9.13
26	9300	85.23	n.d.	n.d.
26	9600	81.02	n.d.	n.d.
26	9900	73.76	n.d.	n.d.
26	10260	65.77	n.d.	n.d.
26	10620	59.69	n.d.	n.d.
26	10980	54.11	n.d.	n.d.
26	11340	50.00	n.d.	n.d.
26	11700	46.79	58.58	n.d.
26	12300	42.20	n.d.	n.d.
26	13200	39.13	n.d.	3.45
26	14100	37.87	4.32	4.03
26	15600	36.16	3.75	0.93
26	17100	35.20	6.50	2.51
26	18660	34.74	9.77	0.51
26	21000	34.23	5.27	0.54
26	23700	34.07	0.01	n.d.

Appendix F. Solute and fine particle concentrations observed at the downstream sampling station
(92 m) during the December injection experiment

Distance Downstream (m)	Time	Observed Cl (ppm)	Phosphate (ppb)	Particles (#/uL)
92	240	34.55	n.d.	n.d.
92	540	34.60	n.d.	n.d.
92	840	34.59	n.d.	n.d.
92	1380	34.59	n.d.	n.d.
92	1680	34.55	n.d.	n.d.
92	1980	34.49	n.d.	n.d.
92	2280	34.42	8.10	n.d.
92	2580	34.48	n.d.	n.d.
92	2700	34.77	n.d.	2.01
92	2880	36.34	n.d.	n.d.
92	3060	40.07	23.11	0.84
92	3180	45.69	n.d.	n.d.
92	3360	58.90	85.52	4.82
92	3540	73.50	n.d.	n.d.
92	3660	87.07	190.19	n.d.
92	3840	110.72	n.d.	n.d.
92	3960	124.93	321.53	6.76
92	4140	153.30	n.d.	n.d.
92	4260	166.53	385.47	6.30
92	4440	191.59	n.d.	12.90
92	4560	206.69	455.26	20.49
92	4680	225.03	n.d.	12.69
92	4860	250.60	661.29	26.87
92	5040	271.02	731.23	10.68
92	5160	288.20	925.16	12.72
92	5400	313.95	772.34	14.63
92	5640	338.76	973.24	17.74
92	5880	352.73	940.83	19.29
92	6120	364.31	n.d.	16.21
92	6360	372.70	1007.02	n.d.
92	6780	390.60	n.d.	n.d.
92	7080	405.75	1111.38	16.21
92	7320	419.25	1130.58	26.56
92	7560	430.16	1085.68	24.36
92	7860	431.65	n.d.	n.d.
92	8220	412.05	1179.03	15.78
92	8400	392.02	1082.07	26.65
92	8580	370.33	1238.15	14.08
92	8760	346.44	n.d.	n.d.
92	9000	309.51	896.15	10.05
92	9180	284.50	n.d.	n.d.
92	9360	261.31	747.04	13.68
92	9540	238.73	n.d.	n.d.
92	9720	221.89	603.48	3.68
92	9960	198.68	n.d.	n.d.
92	10140	185.65	514.72	7.07
92	10320	171.28	n.d.	n.d.
92	10500	160.53	416.32	1.78
92	10680	148.92	n.d.	n.d.
92	10860	140.42	362.77	4.55
92	11040	131.95	n.d.	n.d.
92	11280	121.19	297.13	3.30
92	11520	111.88	n.d.	n.d.
92	11760	104.07	n.d.	n.d.
92	12300	88.39	215.12	n.d.
92	12900	74.25	151.52	2.68
92	13800	58.93	105.53	n.d.
92	14700	49.38	66.90	6.02
92	15600	49.38	49.07	2.89
92	16500	43.87	16.65	6.68
92	18300	41.40	16.54	2.81
92	20100	36.99	12.78	1.43
92	22620	42.19	22.41	n.d.

Appendix H. Particle distribution between sediment and vegetation.

Sample		Estimated particles in sed per 1 m ² of stream (x 10 ⁷)	# Particles in sed over reach area (averaged) (x 10 ⁹)	Estimated particles in veg per 1 m ² of stream (x 10 ⁸)	# Particles in veg over reach area (averaged) (x 10 ⁹)	Total # particles entering upstream reach (x 10 ⁹)	Estimated fraction of particles in sed/ total particles	Fraction of particles in veg/total particles
Fall	e3s1	58.63	2.62	43.53	1.82	7.77	0.3	0.2
	e3s2	24.79		9.88				
	e3s3	12.83		7.25				
	e3s4	5.54		0.90				
Summer	e2s1	62.71	1.70	71.93	1.54	7.64	0.2	0.2
	e2s2	1.17		15.15				
	e2s3	1.75		46.40				
	e2s4	0.58		1.75				
Spring	e1s1	11.96	0.99	2.93	1.82	4.13	0.2	0.4
	e1s3	7.29		0.60				